

Water-Soluble α -Amino Acid Complexes of Molybdenum as Potential Antidotes for Cyanide Poisoning: Synthesis and Catalytic Studies of Threonine, Methionine, Serine, and Leucine Complexes

Johanna M. Gretarsdottir, Sigridur Jonsdottir, William Lewis, Trevor W. Hambley, and Sigridur G. Suman*



Cite This: <https://dx.doi.org/10.1021/acs.inorgchem.0c02672>



Read Online

ACCESS |



Metrics & More

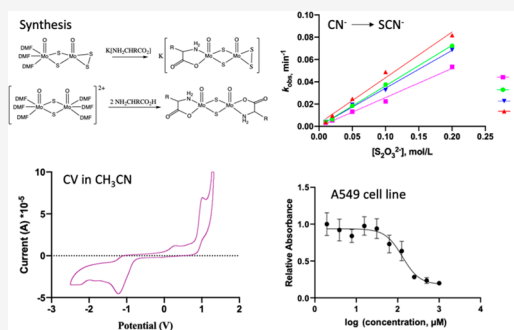


Article Recommendations



Supporting Information

ABSTRACT: Water-soluble complexes are desirable for the aqueous detoxification of cyanide. Molybdenum complexes with α -amino acid and disulfide ligands with the formula $K[(L)Mo_2O_2(\mu-S)_2(S_2)]$ ($L = \text{leu}$ (**1**), met (**2**), thr (**3**), and ser (**4**)) were synthesized in a reaction of $[(DMF)_3MoO(\mu-S)_2(S_2)]$ with deprotonated α -amino acids; leu, met, thr, and ser are the carboxylate anions of L-leucine, L-methionine, L-threonine, and L-serine, respectively. Potassium salts of α -amino acids (leu (**1a**), met (**2a**), thr (**3a**), and ser (**4a**)) were prepared as precursors for complexes **1–4**, respectively, by employing a nonaqueous synthesis route. The ligand exchange reaction of $[Mo_2O_2(\mu-S)_2(DMF)_6](I)_2$ with deprotonated α -amino acids afforded bis- α -amino acid complexes, $[(L)_2Mo_2O_2(\mu-S)_2]$ (**6–8**). A tris- α -amino acid complex, $[(\text{leu})_2Mo_2O_2(\mu-S)_2(\mu-\text{leu} + H)]$ (**5**; leu + H is the carboxylate anion of L-leucine with the amine protonated), formed in the reaction with leucine. **5** crystallized from methanol with a third weakly bonded leucine as a bridging bidentate carboxylate. An adduct of **8** with SCN^- coordinated, **9**, crystallized and was structurally characterized. Complexes **1–4** are air stable and highly water-soluble chiral molecules. Cytotoxicity studies in the A549 cell line gave IC_{50} values that range from 80 to 400 μM . Cyclic voltammetry traces of **1–8** show solvent-dependent irreversible electrochemical behavior. Complexes **1–4** demonstrated the ability to catalyze the reaction of thiosulfate and cyanide *in vitro* to exhaustively transform cyanide to thiocyanate in less than 1 h.



INTRODUCTION

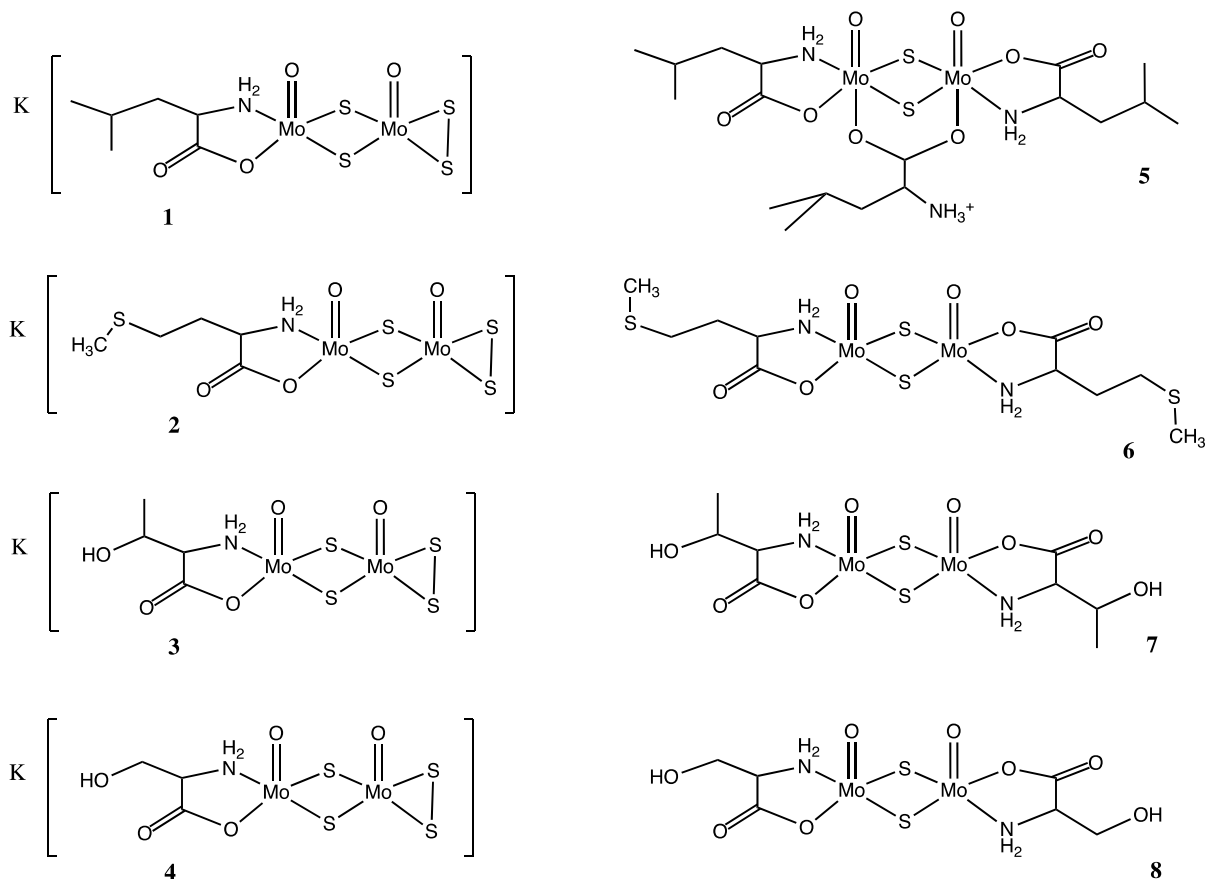
Cyanide has received increased attention as a toxin in inhalation injuries in recent years.^{1–4} The largest risk of cyanide poisoning for the general public is through exposure to smoke inhalation from residential, industrial, and forest fires.^{5,6} Hydrogen cyanide (HCN) is formed in an incomplete combustion of organic materials containing nitrogen, such as the common materials silk, wool, nylon, and many plastics (e.g., melamine, polyurethane, and polyacrylonitrile).⁷ The accidental volatilization of HCN is a potential source of cyanide poisoning in industry.^{8,9} Cyanide salts are common starting materials in the chemical industry for chemical synthesis and are a key ingredient in metal processing.¹⁰ Acute poisoning can result if these salts come into contact with moisture and instantaneously form HCN.¹¹ The acute toxicity of cyanide^{12,13} calls for a highly efficient approach and a rapidly administrable treatment for cyanide poisoning.^{14,15}

Cyanide is a noncompetitive inhibitor of cytochrome c oxidase, halting cellular respiration and resulting in hypoxic anoxia.² Cyanide is an endogenous molecule¹⁶ that is metabolized *in vivo* by the rhodanase sulfurtransferase enzyme. Rhodanase catalyzes the sulfur transfer from sulfur donor substrates to cyanide, forming thiocyanate that is excreted in urine.¹⁷ The reaction of thiosulfate and cyanide is currently a

treatment for cyanide poisoning, where thiosulfate acts as a sulfur donor to the rhodanase enzyme *in vivo*.¹⁸ At lethal doses, the activity of rhodanase is not sufficient to detoxify the cyanide.² Transition metal complexes able to catalyze the reaction of cyanide and sulfur donor substrates (e.g., thiosulfate) are an attractive option in the development of novel emergency treatments for cyanide poisoning *in vivo*. The development of catalytic molybdenum metallodrugs to supplement rhodanase places the need for a low cytotoxicity and good physical properties, such as the water solubility of the potential therapies, at the forefront of challenges to overcome.^{19,20} The selection of ligands and counter cations for the molybdenum complexes affect both the solubility and toxicity of the potential treatment.²¹

Received: September 7, 2020

Chart 1. Structures of Complexes 1–8



Molybdenum is one of the more abundant elements on the planet, and enzymes containing molybdenum at their active site appear to be present in all forms of life.^{22,23} At least 50 enzymes are known;^{24,25} among them, xanthine oxidase and sulfite oxidase are well-known molybdoenzymes in humans.²⁶

The ability of molybdenum with S_n^{2-} ($n = 1-4$) ligands to accept or donate sulfur atoms has been exploited for sulfur removal in hydrodesulfurization processes (HDS).²⁷ In this mechanism, the sulfur reacts with a “ MoS_2 ” moiety in a heterogeneous reaction to insert into $Mo-S$ bonds or oxidatively add to the metal. Dinuclear molybdenum complexes with α -amino acid donors have also been shown to be effective catalytic precursors for epoxidations.²⁸ The ability of the “ $Mo(O)(S)$ ” moiety to donate sulfur to other substrates was demonstrated in the reaction of $[LPrMoOS(OPh)]$ with $(Et_4N)CN$ in acetonitrile, producing $[LPrMoO(MeCN)(OPh)]$ ($LPr = \text{hydrotris}(3\text{-isopropylpyrazol-1-yl})\text{borate}$) and SCN^- .²⁹ Similarly, the $Mo=O$ bond also reacts with sulfur containing substrates, such as thiosulfate.³⁰

The terminal sulfido group on molybdenum reacts in stoichiometric reactions with cyanide to form thiocyanate in a reaction commonly employed to model the reactivity and inactivation of molybdenum hydroxylases as well as other molybdoenzymes.^{29,31-34} Molybdenum–cyano complexes were reviewed recently,³⁵ and the reaction chemistry of molybdenum sulfur compounds with cyanide was reported earlier.^{36,37} Most recently, binuclear molybdenum complexes with the “ $Mo(O)(\eta^2-S_2)$ ” moiety in $[Mo_2O_2(\mu-S)_2(S_2)(DMF)_3]$ were shown to react with CN^- to form SCN^- in stoichiometric amounts.³⁸ The complex catalyzes the reaction of thiosulfate and cyanide,

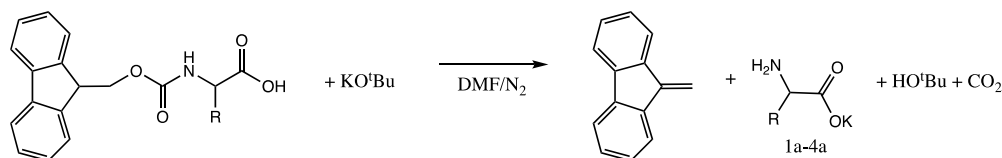
forming sulfite and thiocyanate. The rate of thiocyanate formation is dependent on the thiosulfate concentration, and the reaction proceeds to completion over time.

Although $[Mo_2O_2(\mu-S)_2(S_2)(DMF)_3]$ has shown catalytic activity in the reaction of cyanide with thiosulfate, it is not suitable as a catalytic treatment *in vivo* due to its toxicity and limited aqueous solubility.²¹ Ligand substitution of the DMF by nontoxic and water-soluble α -amino acid ligands (α -aa) decreases the toxicity of the molybdenum complexes and increases the water solubility. Sodium and potassium salts are relatively nontoxic compared to complexes with alkylammonium salts and show a higher water solubility.²¹ Molybdenum–sulfur complexes with water-soluble α -amino acid ligands and Na^+ or K^+ counter cations are therefore an attractive option to achieve biocompatibility. The gas-phase detection of alkali metal salts of threonine, serine, and methionine has been reported using infrared multiple-photon dissociation (IRMPD) spectroscopy.³⁹⁻⁴⁴ However, they were not isolated. In our work, a general method for the isolation of analytically pure potassium salts of leucine, methionine, threonine, and serine (**1a–4a**, respectively) is reported.

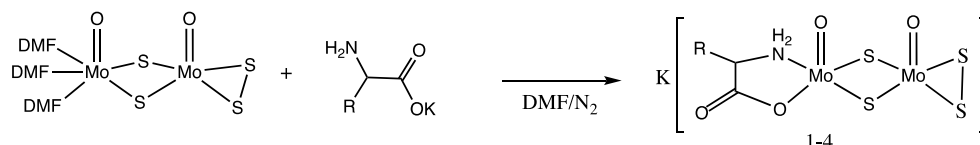
Dinuclear asymmetric molybdenum sulfur complexes (**1–4**) were synthesized using the isolated alkali metal salts as precursors. Bis-amino acid molybdenum sulfur complexes (**6–8**) were synthesized as well as a tris-leucine asymmetric complex (**5**), and their properties investigated.

RESULTS AND DISCUSSION

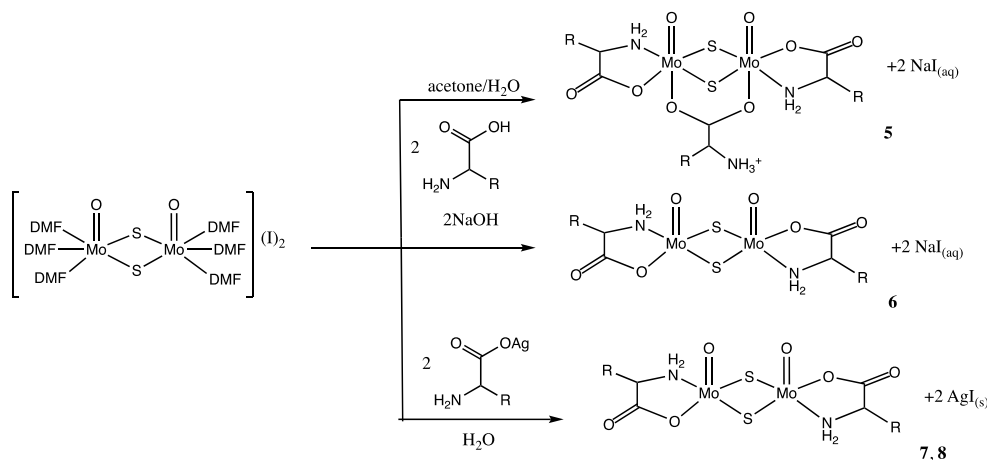
Syntheses. Complexes **1–4** with the α -amino acids leucine, methionine, threonine, and serine, respectively, were synthe-

Scheme 1. Synthesis of Potassium Salts of α -Amino Acids 1a–4a

Scheme 2. Synthesis of Complexes 1–4



Scheme 3. Synthesis of Complexes 5–8



sized in ligand exchange reactions of $[\text{Mo}_2\text{O}_2(\mu\text{-S})_2(\text{S}_2)(\text{DMF})_3]$ with potassium salts of the α -amino acids (Chart 1, 1–4). Neutral complexes were synthesized in reactions of $[\text{Mo}_2\text{O}_2(\mu\text{-S})_2(\text{DMF})_6](\text{I})_2$ with the amino acids (Chart 1, 5–8). A tris- α -amino acid complex with the structure $[\text{Mo}_2\text{O}_2(\mu\text{-S})_2(\mu\text{-leu} + \text{H})(\text{leu})_2]$ (5; leu + H is the carboxylate anion of L-leucine with the amine protonated) formed in the reaction with leucine, while methionine, threonine, and serine formed bis- α -amino acid complexes 6–8, respectively.

The approach used in the synthesis of the mono- α -amino acid complexes is unique to each, while the syntheses of 5–8 drew inspiration from synthetic routes reported for known α -amino acid complexes. Reported procedures for transition metal α -amino acid complexes most often proceed by employing one of the following two methods: (i) reactions of charged complexes with hydrochloride salts of α -amino acids^{45–48} and (ii) reactions of complexes with α -amino acids deprotonated with a base *in situ*.^{49,50}

The reported procedures are incompatible for reactions with complexes possessing the base-labile disulfide ligand in $[\text{Mo}_2\text{O}_2(\mu\text{-S})_2(\text{S}_2)(\text{DMF})_3]$. In this case, isolated salts of α -amino acids are more suitable reagents to prevent a displacement of the disulfide and form water-soluble complexes. While the Na^+ and K^+ salts of glycine are easily isolated using a solid-state method,⁵¹ the same salts of leucine, methionine, threonine, and serine were not able to be isolated using this method. The zwitterionic nature of the amino acids always leads to the

formation of the $\text{NH}_3^+/\text{COO}^-$ pair in water, preventing the isolation of the salts from water.

An alternative method for the synthesis of alkali salts of α -amino acids was employed in a dry aprotic solvent. Potassium salts of α -amino acids (leu (1a), met (2a), thr (3a), and ser (4a)) were prepared as precursors for complexes 1–4 by employing a nonaqueous synthesis route (Scheme 1); leu, met, thr, and ser are the carboxylate anions of L-leucine, L-methionine, L-threonine, and L-serine, respectively. Commercially available Fmoc-protected α -amino acids are highly soluble in DMF and are suitable to facilitate the synthesis in aprotic solvents. The potassium salts of the α -amino acids leucine, methionine, threonine, and serine (1a–4a) were successfully isolated as white solids by the deprotonation of the carboxylic acid of the Fmoc-protected α -amino acids by potassium *tert*-butoxide in dry DMF (Scheme 1). They are very hygroscopic and need to be handled under nitrogen. In the presence of water, the carboxylate group is easily protonated, forming an alkaline solution.

The starting complex, $[\text{Mo}_2\text{O}_2(\mu\text{-S})_2(\text{S}_2)(\text{DMF})_3]$, was synthesized according to a literature procedure.⁵² *In situ* deprotonation in aqueous media is often employed in the synthesis of complexes with amino acid ligands,⁴⁹ resulting in a solution with an alkaline pH. The disulfide ligand of $[\text{Mo}_2\text{O}_2(\mu\text{-S})_2(\text{S}_2)(\text{DMF})_3]$ is sensitive to alkaline pH levels,⁵³ leading to the partial displacement of the disulfide by the incoming ligand L and forming a mixture of complexes with the formulas $[\text{Mo}_2\text{O}_2(\mu\text{-S})_2(\text{S}_2)(\text{L})]^-$ and $[\text{Mo}_2\text{O}_2(\mu\text{-S})_2(\text{L})_2]$; this neces-

sitates the reaction being carried out in the absence of a base. To preserve the disulfide ligand of $[\text{Mo}_2\text{O}_2(\mu\text{-S})_2(\text{S}_2)(\text{DMF})_3]$ in reactions with the amino acid salts, the syntheses of $\text{K}[\text{Mo}_2\text{O}_2(\mu\text{-S})_2(\text{S}_2)(\text{L})]$ (**1–4**) were carried out with dry solvents under nitrogen using standard Schlenk techniques, as shown in Scheme 2. Complexes **1–4** were isolated as solids after aqueous workup and lyophilization. They were isolated as hydrates, as confirmed by IR spectra in anhydrous KBr pellets as well as elemental analysis.

The starting complex $[\text{Mo}_2\text{O}_2(\mu\text{-S})_2(\text{DMF})_6](\text{I})_2$ was synthesized according to a literature procedure.⁵⁴ The structures of the starting complexes revealed the *syn* configuration of the oxo groups, which is preserved unless the sulfide bridge is cleaved at harsh reaction conditions.⁵⁵ The *in situ* deprotonation of the amino acid works well for **5–8**, since the starting material is stable in the reaction conditions. The syntheses of **5** and **6** were carried out in aqueous acetone (Scheme 3) because of the poor aqueous solubility of methionine and leucine. The products were purified by recrystallization from ethanol. Single crystals of **5** suitable for X-ray analysis were obtained after recrystallization from methanol. The silver salt⁵⁶ as well as the sodium and potassium salts⁵¹ of glycine are known. Silver salts of the other α -amino acids may be isolated using an analogous procedure to that used for the glycine salt. The highly water-soluble complexes **7** and **8** were synthesized from $[\text{Mo}_2\text{O}_2(\mu\text{-S})_2(\text{DMF})_6](\text{I})_2$ in a metathesis reaction with the silver salts⁵⁶ of the α -amino acids threonine and serine, respectively, in water (Scheme 3). Insoluble AgI was easily removed by filtration. The crude products of **7** and **8** were purified by recrystallization from water and isolated as solids after lyophilization.

Methionine, threonine, and serine act as bidentate negatively charged chelating ligands toward the $[\text{Mo}_2\text{O}_2(\mu\text{-S})_2]^{2+}$ core to form neutral bis- α -amino acid complexes (Chart 1). Three molecules of leucine reacted consistently with $[\text{Mo}_2\text{O}_2(\mu\text{-S})_2(\text{DMF})_6](\text{I})_2$ to form a neutral tris-leucine complex regardless of the reaction stoichiometry. Two of the leucine ligands act as bidentate N,O-chelates similar to **6–8**. The third leucine is in its zwitterionic form, with a neutral O,O-chelate bridging both molybdenum atoms and the amine group in the protonated $-\text{NH}_3^+$ form. The reaction yield based on leucine was 77%, where it acts as a limiting reagent in this reaction.

α -Amino acids coordinate to metal atoms through various degrees of chelation, where mono-, bi-, tri- and tetradentate coordination modes have been reported.⁵⁷ Bidentate N,O-chelation through the amino and carboxylate groups is typically observed, but the degree of coordination is determined by the nature of the α -amino acids, their side chains, and the coordinated metal. α -Amino acids with simple aliphatic side chains can act as monodentate ligands but are most often bidentate.⁴⁹ The thioether sulfur of methionine is a weak base that favors coordination to select metal ions,⁵⁸ and monodentate S-chelation through the methionine thioether group to Pd has been reported.⁵⁹ Although $[\text{Mo}_2\text{O}_2(\mu\text{-S})_2]^{2+}$ forms a tridentate chelate with cysteine thiolate,⁶⁰ a Mo center rarely coordinates to thioethers, preferably doing so when it is in lower oxidation states such as Mo(II).⁶¹ Methionine therefore most likely acts as a bidentate ligand.⁶² Serine and threonine both have hydroxyl groups in the β -position; however, N,O-chelation is typically observed, and the hydroxyl groups are left pendant due to their relatively high pK_a values.^{59,63,64}

A few dinuclear molybdenum complexes with the $[\text{Mo}_2\text{O}_2(\mu\text{-S})_2]^{2+}$ core and α -amino acid ligands have been reported, such as the symmetric tridentate N,O,S-chelated bis-cysteine complex⁴⁵

with the $[\text{Mo}_2\text{O}_2(\mu\text{-S})_2]^{2+}$ core as well as its S,O-bridged $[\text{Mo}_2\text{OS}(\mu\text{-O})(\mu\text{-S})]^{2+}$,⁴⁷ and O,O-bridged $[\text{Mo}_2\text{O}_2(\mu\text{-O})_2]^{2+}$ counterparts.⁴⁶ The crystal structure of the asymmetric dinuclear bidentate tris-glycine complex $[\text{Mo}_2\text{O}_2(\mu\text{-S})_2(\text{Gly})\text{-}(\text{gly})_2]^{49}$ has been reported, where the glycine coordinates to the Mo center both as a N,O-chelate and an O,O-bridging amino acid. The carboxylate coordinates as a bridging ligand to both Mo centers. Mononuclear Mo(VI) peroxo (O_2^{2-}) complexes have been crystallized as $[\text{MoO}(\text{O}_2)_2(\alpha\text{-aa})(\text{H}_2\text{O})]$ with glycine, alanine, and proline.⁶⁵ The glycine, alanine, and proline complexes were isolated with the amino acid as monodentate O-bonded ligands to the Mo center as expected, since Mo(VI) has a preference for oxygen coordination over nitrogen coordination. The same researchers reported additional complexes with valine, leucine, serine, asparagine, and glutamine without structural data.⁶⁵

Structural Analysis of 5. Complex **5** crystallized from a methanol solution with two methanol molecules in the space group $P4_3$. The complex is the S,S,S-isomer, with the N,O- and O,O-coordinated ligands in the S-orientation. The NH_2 and O donor groups are in *trans*-orientations in the equatorial plane. The molecular structure of **5** is shown in Figure 1, and a summary of crystal and structural refinement data is presented in SI Table 1; selected bond distances and bond angles are presented in SI Tables 2 and 3.

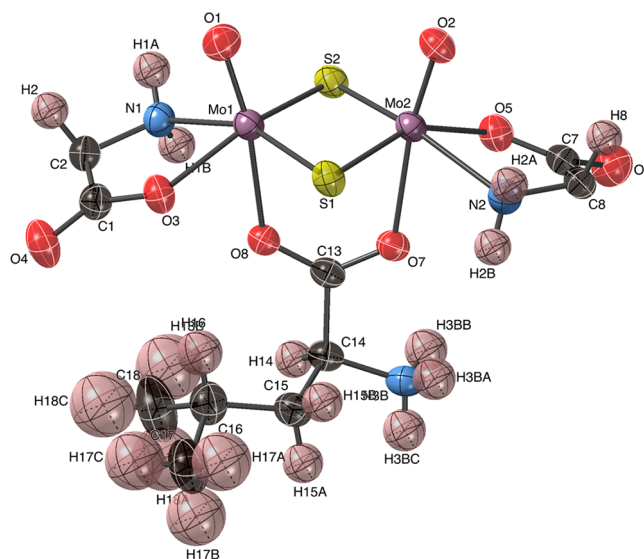


Figure 1. Structure and labeling of **5**. The side chains on C2 and C8 are omitted for clarity.

The complex contains two octahedra sharing the sulfide-bridge line. Two coordination modes of leucine were observed; a leucine was chelated to each molybdenum atom via its amine nitrogen atom and an α -carboxylate oxygen atom. The third leucine acted as an O,O-bridging donor to the two molybdenum atoms through its carboxylate oxygen atoms. Two sulfur atoms and a terminal oxygen atom complete the octahedral moiety around each molybdenum atom. The $[\text{Mo}_2\text{O}_2(\mu\text{-S})_2(\text{leu})_2]$ moiety of **5** is near symmetrical with a C_2 rotation axis, but the bridging leucine imposes a C_1 symmetry on the complex.

The structure of **5** is similar to that of $[\text{Mo}_2\text{O}_2(\mu\text{-S})_2(\text{cys})_2]^{2-}$ where the Mo–N (average of 2.215(4) Å) and Mo=O (average of 1.678(3) Å) bond distances are similar and unexceptional.⁶⁰ The carboxylate oxygens of the N,O-coordinated leucine are

located in the equatorial plane in **5** as opposed to in the axial positions in $[\text{Mo}_2\text{O}_2(\mu\text{-S})_2(\text{cys})_2]^{2-}$. The Mo–O bonds to the bridging leucine (average 2.304 Å) are longer than the Mo–O bonds from the chelated leucines (average 2.097 Å), presumably because of the *trans*-influence from the Mo=O group, but the Mo(1)–O(8) and Mo(2)–O(7) bond distances are similar to the axial bond distances in $[\text{Mo}_2\text{O}_2(\mu\text{-S})_2(\text{cys})_2]^{2-}$.⁶⁰

The C–O bond distances in the bridging carboxylate are in agreement with its deprotonated bridging coordination. The other two carboxylates in the complex exhibit differences in the C–O and C=O bond distances for C(1)–O(3) and C(1)–O(4) and C(7)–O(5) and C(7)–O(6), respectively, that are less than 0.1 Å, as has also been observed for $[\text{Mo}_2\text{O}_2(\mu\text{-S})_2(\text{citrate})_2]^{6-}$.⁶⁶ The bond angles in the bridging carboxylate are all wider than 120°, which is likely imposed by the geometry of the $[\text{Mo}_2(\text{O})_2(\mu\text{-S})_2]^{2+}$ core. The Mo(1)–Mo(2) bond distance is 2.8285(5) Å, or similar to those seen for $[\text{Mo}_2\text{O}_2(\mu\text{-S})_2(\text{cys})_2]^{2-}$ ⁶⁰ and $[\text{Mo}_2\text{O}_2(\mu\text{-S})_2(\text{citrate})_2]^{6-}$.⁶⁶ The dihedral angle of the $[\text{Mo}_2\text{O}_2(\mu\text{-S})_2]^{2+}$ core was calculated as 173°, or quite a bit wider than those in $[\text{Mo}_2\text{O}_2(\mu\text{-S})_2(\text{DMF})_6](\text{I})_2$,⁵⁴ $[\text{Mo}_2\text{O}_2(\mu\text{-S})_2(\text{S}_2)(\text{DMF})_3]$,⁵² and $(\text{Me}_4\text{N})_2[\text{Mo}_2\text{O}_2(\mu\text{-S})_2(\text{S}_2)_2]$ ⁶⁷ that fall between 150° and 160°.

Structural Analysis of 9. Complex **8** crystallized as the SCN^- adduct **9** in the space group $P\bar{3}c1$ from an ethanol solution containing a mixture of KSCN and $\text{Bu}_4\text{N}^+\text{SCN}^-$ and is labeled **9** to distinguish it from **8**. The complex has a C_2 symmetry, and the thiocyanato groups are *trans* to each other; the molybdenum atoms are in a highly distorted octahedral geometry. The bidentate serine ligands have the nitrogen donors *trans* to each other in the equatorial plane, and the carboxylate oxygen is in a *trans*-orientation to the Mo=O group. The molecular structure of **9** is shown in Figure 2, and a summary of the crystal and structural refinement data is presented in SI Table 1 as well as selected bond distances and bond angles in SI Tables 4 and 5.

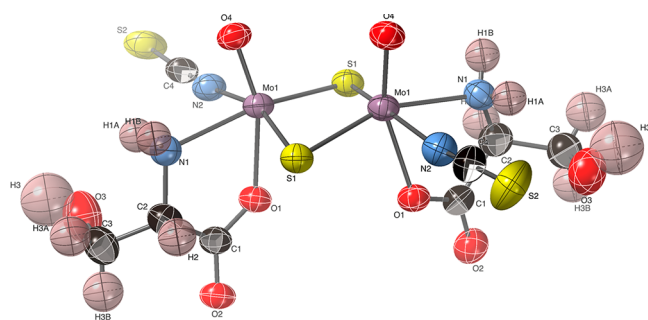


Table 1. Selected IR Bands of 1–8 (cm⁻¹)

complex	$\nu(\text{Mo}=\text{O})$	$\nu(\text{Mo}-\text{S}_\text{b})$	$\eta^2\text{-S}_2$	$\nu(\text{C}=\text{O})$ <i>asym</i>	$\nu(\text{C}=\text{O})$ <i>sym</i>	$\delta(\text{NH}_3^+)$
$\text{Mo}_2\text{O}_2(\mu\text{-S})_2(\text{S}_2)(\text{DMF})_3^a$	954(s) 947(s)	467(m)	527 (w)			
1	946 (s)	467 (m)	520 (w)	1609 (s)	1387 (m)	
2	945 (s)	467 (m)	520 (w)	1617 (s)	1377 (m)	
3	942 (s)	466 (m)	520 (w)	1625 (s)	1385 (m)	
4	943 (s)	467 (m)	521 (w)	1624 (s)	1383 (m)	
5	952 (s) 943 (s)	464 (m)		1655 (s) 1617 (s)	1389 (m) 1377 (m)	1575 (m) 1517 (m)
6	944 (s)	464 (m)		1644 (s)	1374 (m)	
7	943 (s)	464 (m)		1640 (s)	1382 (m)	
8	940 (s)	460 (m)		1624 (s)	1385 (m)	

^aFrom ref 54

displays a lower energy for the antisymmetric band compared to the 2:1 series. 4 and 8 were found to have virtually the same carboxylate bands, although the band was broad in both complexes. Complex 5 also displays an additional band at 1575 cm⁻¹ due to bending modes of the free NH₃⁺ group.

Electronic Spectra. Electronic spectra of 4 and 8 in H₂O are shown in Figure 3. They are representative of the spectra of the

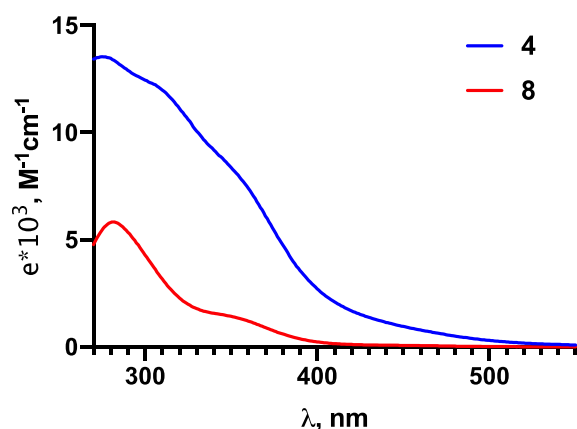


Figure 3. UV-vis spectra of 4 and 8 in H₂O.

mono- and bis- α -amino acid complexes shown with the same amino acid ligand. The electronic spectrum of 4 exhibits a charge transfer band (π)S \rightarrow (d)Mo of the four-membered ring “Mo₂S₂” with a maximum at 274 nm and shoulders at 305 and 347 nm from $d-d$ transitions of the central metals, which are consistent with previous reports.^{47,49,69}

A weak absorbance at 474 nm was observed that was associated with $n-\pi^*$ transition in the disulfide ligand.⁶⁹ This absorbance is absent in the spectrum of 8, as expected. The electronic spectrum of 8 exhibits a charge-transfer band with a maximum at 281 and a shoulder at 350, which are analogous to the bands observed for 4.

There is no distinguishable difference in the electronic spectrum of the tris- α -amino acid complex 5 and the spectra of the bis- α -amino acid complexes 6–8. Most likely, the bridging leucine ligand dissociates in solution. The complexes 1–4 are an intensely bright orange color, while 5–8 are light orange to pale yellow. In complexes 5–8, the disulfide ligand, which is a donor or acceptor ligand that gives rise to charge transfer bands, was exchanged for amino acid ligands that predominantly serve as σ -

donors, resulting in reduced charge-transfer band intensities in 5–8 compared to those in 1–4.

Mass Spectrometry. The ESI mass spectra of the molybdenum complexes were obtained in the negative scan mode. Either acetonitrile or methanol was used as the solvent. Simulations of the isotope pattern expected for the mono-anion match the observed major peaks in the measured spectra of the complexes (SI Figures 1–16). The isotope pattern and exact mass were compared for the measured versus simulated mass. The measured and simulated peaks reported show an excellent match for the isotope pattern and a variation in the m/z less than 2 ppm for 1–8. The values are reported in the Experimental Section. The mass spectra of 1–4 exhibit a peak for the anion $[\text{Mo}_2\text{O}_2(\mu\text{-S})_2(\text{S}_2)(\text{L})]^-$. The ESI mass spectra of 6–8, $[\text{Mo}_2\text{O}_2(\mu\text{-S})_2(\text{L})_2]$, exhibit a peak for the mono-anion $[(\text{L})_2\text{Mo}_2\text{O}_2(\mu\text{-S})_2 - \text{H}^+]^-$. Similarly, the mass spectrum of 5 exhibits a peak for the anion $[(\text{leu})_2\text{Mo}_2\text{O}_2(\mu\text{-S})_2(\mu_2\text{-leu} + \text{H}) - \text{H}^+]^-$ as well as a peak for the anion $[(\text{leu})_2\text{Mo}_2\text{O}_2(\mu\text{-S})_2 - \text{H}^+]^-$. The second peak in the mass spectrum of 5 was observed because one leucine dissociated during the measurement.

Physical Properties. Water Solubility. The water solubility of 1–8 was quantified, and the results are presented in Table 2. The solubilities of 1–8 were compared to those of $[\text{Mo}_2\text{O}_2(\mu\text{-S})_2(\text{S}_2)(\text{DMF})_3]$ and $(\text{Et}_4\text{N})_2[\text{Mo}_2\text{O}_2(\mu\text{-S})_2(\text{S}_2)(\text{S}_4)]$. All of the complexes included have the $[\text{Mo}_2\text{O}_2(\mu\text{-S})_2]^{2+}$ core.

Complexes 1–4 all demonstrate a higher water solubility than that of $[\text{Mo}_2\text{O}_2(\mu\text{-S})_2(\text{S}_2)(\text{DMF})_3]$. Substitution of the DMF ligands with threonine or serine ligands (3 and 4, respectively) increases the water solubility over 6-fold. The exchange of DMF with leucine and methionine ligands (1 and 2, respectively)

Table 2. Water Solubility for Complexes 1–8 and the Starting Materials

complex	water solubility (g/L)
1	11.4
2	4.2
3	22.2
4	24.5
5	4.9
6	8.1
7	>200 ^b
8	197
$[\text{Mo}_2\text{O}_2(\mu\text{-S})_2(\text{S}_2)(\text{DMF})_3]$	3.5 ^a
$(\text{Et}_4\text{N})_2[\text{Mo}_2\text{O}_2\text{S}_8]$	1.0 ^a

^aFrom ref 21. ^bThe solution became viscous at 200 g/L.

increases the water solubility less dramatically than in the case of threonine and serine substitutions, mostly because methionine and leucine themselves are less hydrophilic.⁷⁰ The aqueous solubility of the free threonine was reported as 106 g/L, and that of serine was reported up to 250 g/L. The complexes 1–4 do not demonstrate the same order of solubility as the free amino acids, where methionine has higher water solubility than leucine. The hydroxyl groups in the side chains of threonine and serine increase the water solubility, while methionine and leucine have more aliphatic properties. A similar increase in the solubility was also observed for the neutral complexes (5–8). The bis-threonine complex (7) demonstrated such a high water solubility that it proved impossible to obtain a saturated solution. No precipitate was observed when the experiment was carried out, and the solution became viscous when efforts were made to obtain a saturated solution. The bis-serine complex (8) was also highly water-soluble. The bis-leucine (5) and bis-methionine (6) complexes showed lower solubilities than their disulfide complex equivalents (1 and 2, respectively).

The fact that the bis-amino acid complexes 7 and 8 show higher water solubilities than their corresponding disulfide potassium salts suggests that the incorporation of highly water-soluble ligands plays a more significant role in increasing the water solubility than adding a water-soluble counteranion. Strong intermolecular S...S interactions can negatively impact the solubility of compounds with the "Mo₂O₂(μ-S)₂(S₂)" moiety, where the disulfide sulfur atoms may interact with a bridging sulfur atom in another molecule.⁶⁹ Complexes 2 and 6 are therefore likely to have comparably low solubilities. The leucine complexes 1 and 5 are appreciably organo-soluble, and the water solubility of 1 is likely determined by the potassium counteranion. Aliphatic tetraethylammonium cations result in the lower water solubility of (Et₄N)₂[Mo₂O₂S₈], which was less than a third than that of the structurally similar [Mo₂O₂(μ-S)₂(S₂)(DMF)₃]. The choice of counteranions therefore can play a significant role in solubility of transition metal complexes and was given careful consideration.²¹

Cytotoxicity. Cytotoxicities were determined in the A549 lung cancer cell line by the MTT method for all complexes except 5, which was insufficiently soluble in the media employed. The IC₅₀ values are given in Table 3 and cover a

Table 3. IC₅₀ Values Determined for 1–4 and 6–7 in the A549 Cell Line at 72 h^a

compound	IC ₅₀ (mM)
cisplatin	0.008(2)
1	~0.25
2	~0.25
3	~0.25
4	0.12(4)
6	0.08(3)
7	~0.40
8	0.14(4)

^aCisplatin is given as a reference.

range from 80(3) to about 400 μM, with all plots of activity versus growth that plateaued doing so at 20% or more of the activity of the controls (SI Figure 17). The leucine (1) and threonine (3 and 7) complexes as well as one of the methionine complexes (2) are the least toxic, with IC₅₀ values in the range of 250–400 μM. The serine complexes (4 and 8) and the other methionine complex (6) have similar activities, with 6 being the

most active with an IC₅₀ of about 80(3) μM and a plateau at about 20%. In the same assay, cisplatin has a cytotoxicity of 8(2) μM, which is consistent with values reported in the literature.⁷¹ It is not clear what is responsible for the difference in toxicities, but given the lack of systematic variation with the amino acid or structure it is most likely related to the rate and extent of cellular accumulation. If so, the lower toxicity, while desirable, may correlate with a lower capacity to react intracellularly with cyanide. However, given that the uptake of 3 is high⁷² and its toxicity is low, all compounds are likely to be able to accumulate to high levels without inducing significant cell death.

Cyclic Voltammetry. The electrochemistry of selected complexes was explored in CH₃CN. The cyclic voltammograms were run for 2 mM solutions of 1–8 in CH₃CN and 0.2 M in solutions in Bu₄NPF₆. Ag/AgCl₂ was used as the reference electrode. The data are summarized in Table 4.

Table 4. Cyclic Voltammetry Data for 1–8^a

complex	E _{ox1} (V)	E _{ox2} (V)	E _{red1} (V)
1	0.278		-1.13
2	0.347		-1.13
3	0.304		-1.16
4	0.361		-1.25
5	0.336	1.02	-1.18
6	0.363	1.05	-1.14
7	0.255	1.01	-1.21
8	0.303	1.03	-1.24

^aReported versus the Ag/AgCl reference electrode; CH₃CN, 0.1 V/s.

The [Mo₂O₂(μ-S)₂]²⁺ core with various ligands has been explored electrochemically in aqueous media⁴⁷ and aprotic media.^{73,74} The electrochemical behavior was reported to differ significantly based on the experimental conditions. The [Mo₂O₂(μ-S)₂]²⁺ core is robust under neutral or acidic conditions⁷⁵ and unlikely to cause ROS generation *in vivo*. Reported aqueous electrochemical events for [Mo₂O₂S₂(cys)₂]²⁻ were concluded to be proton-coupled electron transfer steps (PCET)⁷⁶ are apparently capable of reducing the two Mo centers in a single step,⁷⁷ while the reductions in aprotic solvents were found to proceed stepwise.⁷³ The study of the electrocatalytic properties of [Mo₂O₂S₂(cys)₂]²⁻ and related complexes attributed the observed catalytic properties to the [Mo₂O₂(μ-S)₂]²⁺ core and revealed a minimal influence by the ligands employed,⁷⁸ whereas changing from aryl to alkyl ligands had a larger impact than changing the donor atoms.⁷⁷ Influences from the ligand donor sets of 1–8 were mostly observed in shifts of the oxidation and reduction potentials rather than in new peaks. Consequently, the cyclic voltammograms of 1–4 (Figure 4) with a chemically reactive disulfide ligand were expected to look similar to those of 5–8 (Figure 5), and electrochemical differences between 1–8 were not expected to be remarkable since the donor atoms and ligand properties were similar.

The two Mo(V) centers can be oxidized to two Mo(VI) centers by a total of two electrons or reduced to two Mo(III) centers by total of four electrons. A single-step two-electron reduction in CH₃CN can lead to cleavage of the Mo–Mo bond and structural rearrangement without compositional change, as was reported for [Mo₂(μ-SR)₂(CO)₈]^{0/2-}.⁷⁹ Two-electron oxidation may lead to two different forms; either two Mo(VI) centers or the disulfide bridge can form an S–S bond. The S–S bond possibility evaluated by DFT calculations for γ-

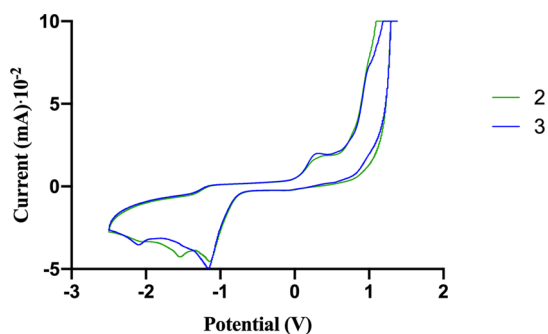


Figure 4. Cyclic voltammograms of 2 and 3 in CH₃CN.

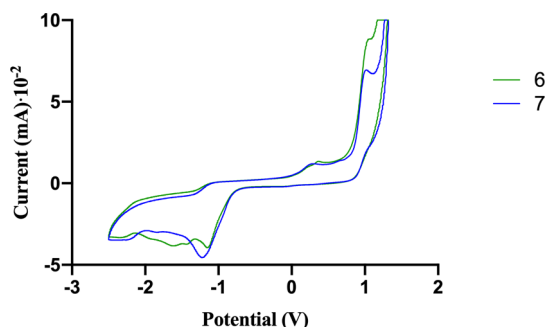


Figure 5. Cyclic voltammograms of 6 and 7 in CH₃CN.

[SiW₁₀Mo₂O₂(μ-S)₂]ⁿ⁻ clusters with C_{2v} symmetry was concluded as unlikely because of its higher energy compared to the Mo(VI) form.⁸⁰ Based on reported electrochemical behavior of related dinuclear cores, one- or two-electron reduction waves could be expected for 2 or 4 electrons, respectively, in 1–8 as well as one two-electron oxidation wave or two one-electron oxidations for a stepwise process. The cyclic voltammetry traces of 1–8 in CH₃CN confirmed that they do not show a large variation in their electrochemical behavior (Figures 4 and 5 and SI Figures 18 and 19).

In CH₃CN, the cyclic voltammograms of 1–8 show an irreversible oxidation in the range from +0.255 V to +0.361 V, and a second poorly defined irreversible oxidation wave at ~1.0 V (Table 4 and Figures 4 and 5) was observed for 5–8. A strong reduction that also appears irreversible was found in the range of –1.13 V to –1.25 V. The lowest oxidation potentials (*E*_{ox1}) were observed for the leucine complex, followed by threonine and methionine, and the highest was observed for the serine complex (Table 4). These potentials are inversely ordered with respect to catalytic reactivity of 1–4 toward cyanide (see *Reactivity with Cyanide*). The peak-current ratios of the oxidation *E*_{ox1} and *E*_{red1} in Table 4 are between 3 and 4 for 1–8, suggesting that the reduction is at least a two-electron process.

Preliminary scans in DMF show the visually comparable electrochemical behavior of 1–8 with respect to the irreversible oxidations and reductions observed. Electrochemical results for 1–8 in aqueous solutions clearly follow a different path than those in aprotic media. A change of the amino acid ligands

results in small shifts in potentials for the same set of waves, and the disulfide ligand does not appear to significantly impact the electrochemical behavior of the complexes. The aqueous electrochemical behavior of 1–8 is under continued study as it is more complex and requires more detailed experiments.

Reactivity with Cyanide. Stoichiometric Reactions. Cyanide has been used to probe the activity of molybdenum hydroxylases with sulfide ligands where a sulfur may be abstracted by cyanide to form thiocyanate.³¹ The molybdoenzymes are known to produce 1 equiv of thiocyanate in these reactions.³² In model studies, mononuclear Mo(VI) complexes with a S²⁻ terminal ligand undergoes a reductive elimination reaction with cyanide to form Mo(IV) and SCN⁻ under anerobic conditions.²⁹ Similarly, Mo(VI) complexes possessing disulfide (S₂²⁻) ligands undergo an internal redox reaction, form an S²⁻ ligand, donate a sulfur atom to form isonitriles.⁸¹ The reactivity of the disulfide ligand of 1–4 in sulfur abstraction reactions with cyanide was studied. The cyanide carries out a nucleophilic attack on the disulfide ligand, and a sulfido ligand remains on the molybdenum center as shown in Scheme 4.

The reactivity was evaluated by quantifying the thiocyanate formation as a function of time. The respective complexes were dissolved in veronal buffer at pH 7.4, and an excess amount of potassium cyanide was added to the solution at time point *t* = 0. Aliquots were taken from the reaction mixtures at fixed time points, and the samples were developed for a colorimetric quantification of thiocyanate as FeSCN²⁺. Figure 6 shows the thiocyanate reaction yield over a 60 min period in the reaction of 1 and of [Mo₂O₂(μ-S)₂(S₂)(DMF)₃] with cyanide.

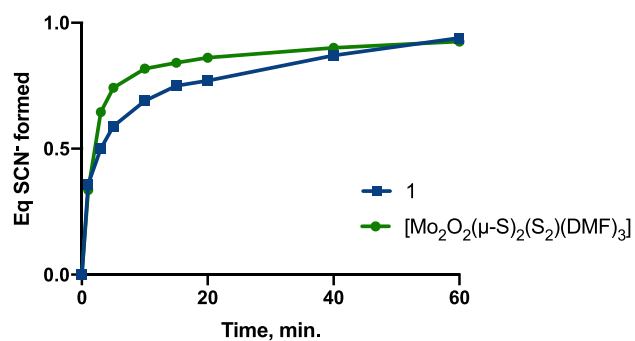


Figure 6. Thiocyanate formation in a reaction of 1 (1 mM) with cyanide (10 mM) compared to SCN⁻ yields from same reaction with [Mo₂O₂(μ-S)₂(S₂)(DMF)₃].

The thiocyanate formation increases rapidly for the first 20 min of the reaction, with about 80% of the thiocyanate of yield formed within this time. Only 1 equiv of thiocyanate was formed, confirming that only one sulfur atom is abstracted from the complex. The results suggest that the complexes are able to convert stoichiometric amounts of cyanide in a relatively quick manner.

Scheme 4. Reaction of 1–4 with 1 equiv of Cyanide



Catalysis of Thiocyanate Formation. The thiocyanate formation in reactions of cyanide and 1–8 in the presence of thiosulfate was quantified as a function of time. The sulfido complex shown in Scheme 4 was assumed to react with thiosulfate, forming sulfite and regenerating the disulfide complex. The kinetic experiments employed the same protocol as the stoichiometric reactions, except excess amounts of thiosulfate in predetermined ratios were added to the complex solution prior to cyanide addition. The thiocyanate yield was quantified by sampling over a 2 h period. Figure 7 shows the thiocyanate reaction yield over a 120 min period, employing 1–4 as catalysts.

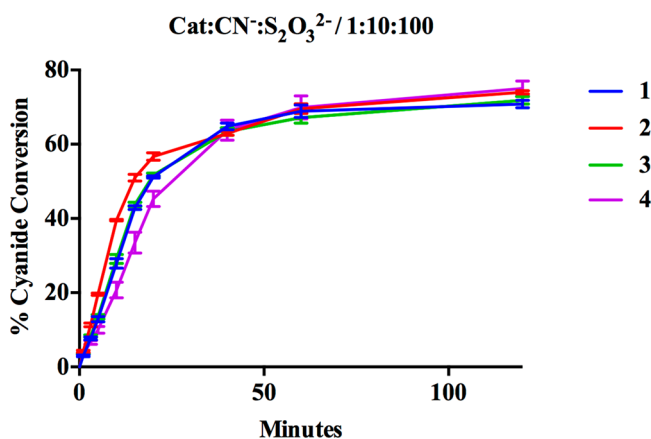


Figure 7. Thiocyanate formation in the reactions of 1–4 (1 mM) with cyanide (10 mM) in the presence of thiosulfate (100 mM).

The reaction rates are dependent on the thiosulfate concentrations. The second-order rate constants for 1–4 were determined at pseudo-first-order reaction conditions and k_{obs} values for several $[\text{S}_2\text{O}_3^{2-}]/[\text{CN}^-]$ ratios plotted. The kinetic plot is shown in Figure 8, and the rate constants are shown in

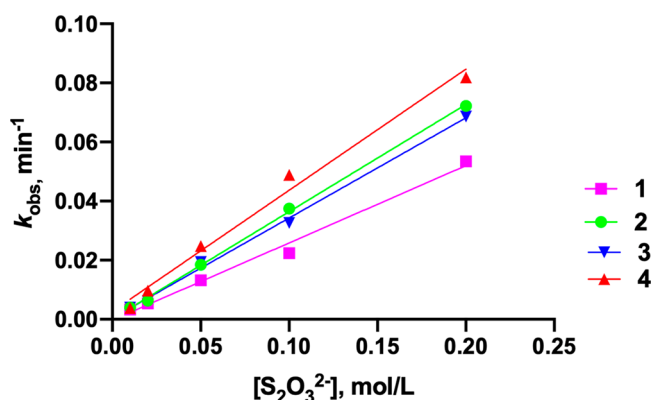


Figure 8. Plot of k_{obs} as a function of variable thiosulfate ratio for 1–4.

Table 5. Second-Order Rate Constants and TOFs for 1–4

compound	k ($\text{M}^{-1} \text{min}^{-1}$)	TOF (min^{-1})
1	0.2615	0.346
2	0.3630	0.560
3	0.3391	0.524
4	0.4100	0.668

Table 5. The results confirm that 1–4 catalyze the reaction of cyanide and thiosulfate to form thiocyanate. Without thiosulfate, the complexes only convert 1 equiv of cyanide to thiocyanate. When 100 equiv of thiosulfate was added, 1–4 converted 45–57% of the cyanide within 20 min. The reduction of a lethal cyanide concentration by 50% *in vivo* over 20 min is sufficient to prevent death from cyanide poisoning.^{1,82–84} While the microscopic mechanism for this reaction is under further study, it can be said that 1–4 appear to follow the same reaction mechanism. The TOF values provided are preliminary, since a rather high catalyst loading was employed and the limits of the system were not verified.

Complexes 5–8 are structurally similar to 1–4 despite lacking the disulfide ligand. The catalytic activity of 5–8 was explored in a similar fashion as that for 1–4 to obtain an insight into the reaction mechanism. The complexes do have open coordination sites on their molybdenum atoms that could potentially serve as catalytically active sites. A possible catalytic reaction mechanism assumes 5–8 catalytically convert cyanide to thiocyanate by a different mechanism where the cyanide interacts with the molybdenum centers and the thiosulfate donates sulfur as a bridging sulfur ligand that is then abstracted by the cyanide. It is nevertheless possible that more than one mechanism takes place in the catalytic conversion of cyanide; potentially, it is a bimetallic mechanism. Thiosulfate was used at a concentration of 200 mM for comparison purposes, as this concentration resulted in high reaction yields for the disulfide complexes.

The bis-amino acid complexes demonstrated catalytic activity in the reaction of cyanide and thiosulfate (SI Figure 20). Compared to the spontaneous reaction of cyanide and thiosulfate (shown in gray in SI Figure 20), reaction yields of thiocyanate were increased significantly in the presence of 5–8. While the spontaneous reaction resulted in the conversion of about 5% of the cyanide within 2 h, a 15–50% conversion was observed in that same time frame in the presence of 5–8. The highest reaction yield was observed for 6, while the lowest reaction yield was observed for 7.

The varying efficiency of these catalysts due to structural differences cannot be explained at this point without further experiments. The disulfide complexes demonstrate higher thiocyanate reaction yields as well as faster conversion rates in the first 20 min. The low initial reaction rates for cyanide conversion catalyzed by 5–8 makes them ill-suited as emergency treatments for cyanide poisoning *in vivo*. The results are nevertheless important as they suggest that open coordination sites on the molybdenum atoms take part in the catalysis with or without the disulfide ligand. Examples of possible mechanisms are (a) cyanide and thiosulfate coordinate to one molybdenum atom each and cyanide carries out a nucleophilic attack on thiosulfate on the opposite molybdenum, releasing thiocyanate, and (b) thiosulfate coordinates in a bidentate fashion (either S-, O-, or O,O-chelation), bridging both molybdenum atoms, and the free cyanide attacks the sulfur donor substrate, releasing thiocyanate. A complex with sulfate bridging two molybdenum atoms has been reported, demonstrating that it is a possible coordination mode for thiosulfate.³⁰ The literature has a single example of a metal catalyzing this reaction,⁸⁵ but it has been explored with the rhodanese enzyme *in vitro*.^{86–88}

Figure 7 reveals about a 10% variance in the catalytic activity of 1–4, which differ only in the R groups of the amino acid ligands. The R group of leucine ($-\text{CH}_2\text{CH}(\text{CH}_3)_2$) is the strongest electron donor of the four, while the R group of serine

($-\text{CH}_2\text{OH}$) is the strongest electron-withdrawing group. The R groups of threonine ($-\text{CH}(\text{CH}_3)\text{OH}$) and methionine ($-\text{CH}_2\text{CH}_2\text{SCH}_3$) have similar electron-donating properties, which fall between those of leucine and serine. The catalytic reaction is initiated with a sulfur atom abstraction reaction from the disulfide ligand by cyanide. The S^{2-} ligand is nucleophilic, and the first sulfur is easily removed.⁵² The serine complex has the fastest initial reaction rate of the four complexes (Table 5), converting 57% of the cyanide to thiocyanate in the first 20 min. The electron-withdrawing properties of the serine ligand side chain reduce the σ -donation of the serine to the $\text{Mo}_2\text{O}_2(\mu\text{-S})_2$ moiety and possibly result in the increased disulfide susceptibility to nucleophilic attack by cyanide. The leucine complex shows the lowest initial reaction rate of the four complexes, converting 45% of the cyanide to thiocyanate in the first 20 min. Its side chain has the largest electron-donating ability, rendering disulfide more electronegative than in the serine complex, and is therefore less reactive in a nucleophilic attack by cyanide. The initial rates of the threonine and methionine complexes fall between those of the serine and leucine complexes, which is in agreement with electron-donating and electron-withdrawing properties of the ligands. The influence of the ligands accounts for at most a 10% difference in the conversion at the 20 min time point, and this is unlikely to be significant in most circumstances.

Up to 75% of the available cyanide was quantified as thiocyanate after a 2 h reaction time for 1–4, and extended sampling did not increase the yields significantly. The remaining 25% and the apparent slowing of the reaction could be caused by catalyst deactivation.⁸⁵ The deactivation of the catalyst could be brought about by cyanide–thiocyanate coordination or the formation of a tetranuclear species through a dimerization reaction of two sulfido complexes.

CONCLUSION

The synthesis of water-soluble α -amino molybdenum–sulfur complexes was successful. The water solubility of the complexes proved highly variable depending on the amino acid ligand employed. The maximum aqueous solubility was found with either alkali metal salts of anionic complexes or amino acid ligands with a hydroxyl group on its side chain. Increasing the aqueous solubility further is desirable in future work, where the results described here show that the ligand solubility contributes more to the overall solubility than the cation. Crystallization was challenging, but complex 5 was crystallized with the carboxylate-bridging zwitterionic form of leucine and the molybdenum centers in an octahedral geometry. 1–4 are chiral compounds, while 5–8 form stereoisomers. The zwitterionic coordination is a route under further study to crystallize additional molecules. The addition of SCN^- to 8 led to the crystallization of 9 with two SCN^- ligands to fill the octahedral coordination around the molybdenum centers. Complexes of this type are subjects for further studies. The electrochemical properties suggest that the $[\text{Mo}_2\text{O}_2(\mu\text{-S})_2]^{2+}$ core is rather inert to redox processes *in vivo*. The ligands employed did not greatly influence the electrochemistry of the core. The cytotoxicity study showed a large range in cytotoxicities that may be explained with further biology experiments, but did show that all compounds have low to very low cytotoxicities.

A reaction with cyanide to produce 1 equiv of thiocyanate proved to be a general reaction for 1–4 with the disulfide ligand, while 5–8 did not react with cyanide in the absence of thiosulfate. Complexes 1–8 all show an ability to bind cyanide, and 1–4 convert it to thiocyanate in a time frame that could be

useful for emergency treatment. The second-order rate constants for the reaction of cyanide and thiosulfate were determined, and the turnover frequency was calculated. The microscopic mechanism for this reaction is under current study. The comparative catalytic abilities for 1–4 show at most a 10% variation with the different amino acid ligands, rendering aqueous solubility and toxicity likely determining factors for a successful detoxification catalyst. Complexes 5–8 were surprisingly active as well, although it is clear they show larger a variation in catalytic activity that is presumably a result of a different mechanism.

The results presented suggest complexes based on the $[\text{Mo}_2\text{O}_2(\mu\text{-S})_2]^{2+}$ core could be both safe and efficient treatments against cyanide poisoning. Next steps include complexes with an increased aqueous solubility; studies of the reaction mechanisms, key steps, and intermediates for these two types of catalysts; and *in vivo* toxicity studies.

EXPERIMENTAL SECTION

Materials. The starting complexes $[\text{Mo}_2\text{O}_2(\mu\text{-S})_2(\text{DMF})_6](\text{I})_2$ ⁵⁴ and $[\text{Mo}_2\text{O}_2(\mu\text{-S})_2(\text{S}_2)(\text{DMF})_3]$ ⁵² were synthesized according to literature procedures. Silver salts of threonine and serine were prepared according to published procedures.⁵⁶ L-Fmoc–Met–OH, L-Fmoc–Leu–OH, L-Fmoc–Thr–OH, and L-Fmoc–Ser–OH·H₂O were purchased from Bachem and used as received. Other reagents, organic solvents, D₂O, and DMSO-*d*₆ were purchased from Aldrich and used as received. DMF, diethyl ether, and acetonitrile were dried and distilled under nitrogen using standard procedures.⁸⁹ Veronal buffer (pH 7.4) was purchased as 5X dilution stock solutions from Lonza. Milli-Q water was used at 18 M Ω /cm or less.

Instrumentation. Infrared spectra were obtained as KBr discs on a Smart Omni-Transmission Nicolet iS10 spectrophotometer at 21 °C. Kinetic measurements and electronic spectra were obtained using either a Varian Cary 100 Bio spectrophotometer or a PerkinElmer Lambda 25 UV–vis spectrophotometer at 21 °C. Mass spectra were recorded using a Bruker microTOF (Bruker autoflex smartbeam) spectrometer as the ESI in negative ion scans. ¹H and ¹³C NMR spectra were recorded on a Bruker 400 Ultrashield spectrometer. Cyclic voltammetric measurements were recorded on an EC Epsilon Eclipse potentiostat/galvanostat. Elemental analyses were obtained from Midwest Microlab, IN.

Preparation of Compounds. General Method for the Synthesis of Potassium Salts of α -Amino Acids. L-Fmoc– α -aa–OH and KO^tBu were dissolved in DMF (50 mL). Upon the addition of DMF, the solution turned red. The reaction was stirred for 22 h, during which time it turned colorless and a white precipitate formed. The precipitate was isolated by filtration and washed with diethyl ether (100 mL). The solid was dried *in vacuo*. The solid was resuspended in acetonitrile, and the mixture was stirred to remove the residual DMF. The product was isolated by filtration and dried *in vacuo*.

$K[\text{C}_6\text{H}_{12}\text{NO}_2]$ (1a). L-Fmoc–Leu–OH (1.51 g, 4.27 mmol) and KO^tBu (0.479 g, 4.27 mmol) yielded in a white powder (0.58 g, 80%). ¹H NMR (DMSO-*d*₆): δ ppm 2.96 (br, $-\text{CH}(\text{NH}_2)-$), 1.66 (m, $(\text{CH}_3)_2\text{CH}-$), 1.44 (m, $-\text{CH}_2-$, 1H), 1.22 (br, $-\text{CH}_2-$, 1H), 0.83 (m, $(\text{CH}_3)_2-$). ¹³C NMR (DMSO-*d*₆): δ ppm 176.08 ($-\text{COO}-$), 54.45 ($-\text{CH}(\text{NH}_2)-$), 44.44 ($-\text{CH}_2-$), 24.54 ($(\text{CH}_3)_2\text{CH}-$), 23.47 ($(\text{CH}_3)\text{CH}(\text{CH}_3)-$), 21.91 ($(\text{CH}_3)\text{CH}(\text{CH}_3)-$). Anal. Calcd for C₆H₁₂KNO₂: C, 42.58%; H, 7.15%; N, 8.28%. Found: C, 42.79%; H, 6.89%; N, 8.14%.

$K[\text{C}_5\text{H}_{10}\text{NO}_2\text{S}]$ (2a). L-Fmoc–Met–OH (2.03 g, 5.47 mmol) and KO^tBu (0.614 g, 5.47 mmol) yielded a white solid product (0.60 g, 58%). ¹H NMR (DMSO-*d*₆): δ ppm 3.06 (s, $-\text{CH}(\text{NH}_2)-$), 2.48 (m, $-\text{SCH}_2\text{CH}_2-$), 2.01 (s, $-\text{CH}_3$), 1.84/1.60 (m/br, $-\text{SCH}_2\text{CH}_2-$). ¹³C NMR (DMSO-*d*₆): δ ppm 174.33 ($-\text{COO}-$), 55.02 ($-\text{CH}(\text{NH}_2)-$), 34.22 ($-\text{SCH}_2\text{CH}_2-$), 30.43 ($-\text{SCH}_2\text{CH}_2-$), 14.60 ($-\text{CH}_3$). Anal. Calcd for C₅H₁₀KNO₂S: C, 32.06%; H, 5.38%; N, 7.48%. Found: C, 32.28%; H, 4.93%; N, 7.01%.

$K[(C_4H_8NO_3)]$ (**3a**). L-Fmoc-Thr-OH (4.06 g, 11.9 mmol) and KOtBu (1.34 g, 11.9 mmol) yielded a white solid (0.85 g, 46%). 1H NMR (DMSO- d_6): δ ppm 3.54 (m, $-CH(OH)-$), 2.88 (br, $-CH(NH_2)-$), 0.94 (d, $-CH_3$). ^{13}C NMR (DMSO- d_6): δ ppm 175.54 ($-COO^-$), 68.37 ($-CH(OH)-$), 58.90 ($-CH(NH_2)-$), 19.06 ($-CH_3$). Anal. Calcd for $C_4H_8KNO_3$: C, 30.56%; H, 5.13%; N, 8.91%. Found: C, 32.00%; H, 5.27%; N, 8.39%.

$K[(C_3H_6NO_3)]$ (**4a**). L-Fmoc-Ser-OH·H₂O (4.09 g, 11.8 mmol) and KOtBu (1.32 g, 11.8 mmol) yielded a white solid (0.95 g, 56%). 1H NMR (DMSO- d_6): δ ppm 3.28 (m, $-CH_2-$), 2.87 (t, $-CH(NH_2)-$). ^{13}C NMR (DMSO- d_6): δ ppm 175.57 ($-COO^-$), 64.97 ($-CH_2-$), 55.24 ($-CH(NH_2)-$). Anal. Calcd for $C_3H_6KNO_3$: C, 25.17%; H, 4.22%; N, 9.78%. Found: C, 26.77%; H, 4.06%; N, 8.63%.

$K[(C_6H_{12}NO_2)Mo_2O_2(\mu-S)_2(S_2)] \cdot H_2O$ (**1**). $[(DMF)_3Mo_2O_2(\mu-S)_2(S_2)]$ (0.51 g, 0.88 mmol) and **1a** (0.15 g, 0.88 mmol) were placed in a Schlenk flask under N₂. Freshly distilled DMF (50 mL) was added to the flask via cannula. The reaction was stirred for 20 h. The red solution was filtered, and the solvent was removed under reduced pressure. The red viscous oil was stirred in diethyl ether (50 mL) overnight until it solidified. The solid was collected by filtration and redissolved in water (60 mL). The solution was filtered and lyophilized. This was repeated until all residual DMF was removed. The product was an orange solid (0.42 g, 92%). UV-vis (H₂O, 7.07×10^{-5} M), λ_{max} (nm): 276 (11083 M⁻¹ cm⁻¹), 305 (10105 M⁻¹ cm⁻¹), 347 (6798 M⁻¹ cm⁻¹), 474 (429 M⁻¹ cm⁻¹). 1H NMR (D₂O): δ ppm 3.70 (br, $-CH(NH_2)-$), 1.65 (br, $(CH_3)_2CHCH_2-$), 0.90 (s, $(CH_3)_2-$). ^{13}C NMR (D₂O): δ ppm 176.88 ($-COO^-$), 53.17 ($-CH(NH_2)-$), 39.62 ($-CH_2-$), 24.08 ($(CH_3)_2CH-$), 21.92 ($(CH_3)CH(CH_3)-$), 20.82 ($(CH_3)CH(CH_3)-$). IR (KBr pellet, cm⁻¹): 3232 (m), 3133 (m, br), 1609 (s), 1387 (m), 946 (s), 520 (w), 467 (m). MS-ESI: $[M - K^+]$ C₆H₁₂Mo₂NO₄S₄ (m/z 485.7757), found m/z 485.7763. Anal. Calcd for C₆H₁₄KMo₂NO₅S₄: C, 13.36%; H, 2.62%; N, 2.60%. Found: C, 12.92%; H, 2.56%; N, 2.18%. $[\alpha]_D^{25}$ (DMF): -6.5° .

$K[(C_5H_{10}NO_2S)Mo_2O_2(\mu-S)_2(S_2)] \cdot H_2O$ (**2**). $[(DMF)_3Mo_2O_2(\mu-S)_2(S_2)]$ (0.46 g, 0.80 mmol) and **2a** (0.15 g, 0.80 mmol) were placed in a Schlenk flask under N₂. Freshly distilled DMF (50 mL) was added to the flask via cannula. The reaction was stirred for 20 h. The clear red solution was filtered, and the solvent was removed under reduced pressure. The red viscous product was stirred in diethyl ether (100 mL) until it solidified. The solid was collected by filtration and redissolved in water (60 mL). The solution was filtered and lyophilized. This was repeated until all residual DMF was removed. The product was an orange solid (0.30 g, 70%). UV-vis (H₂O, 6.84×10^{-5} M), λ_{max} (nm): 275 (11059 M⁻¹ cm⁻¹), 305 (9816 M⁻¹ cm⁻¹), 347 (6317 M⁻¹ cm⁻¹), 474 (450 M⁻¹ cm⁻¹). 1H NMR (D₂O): δ ppm 3.89 (br, $-CH(NH_2)-$), 2.65 (br, $-SCH_2CH_2-$), 2.20 (br, $-SCH_2CH_2-$), 2.15 (s, $-CH_3$). ^{13}C NMR (D₂O): δ ppm 172.63 ($-COO^-$), 53.91 ($-CH(NH_2)-$), 29.62 ($-SCH_2CH_2-$), 28.81 ($-SCH_2CH_2-$), 13.94 ($-CH_3$). IR (KBr pellet, cm⁻¹): 3227 (m, br), 3133 (m), 1617 (s), 1377 (m), 945 (s), 520 (w), 467 (m). MS-ESI: $[M - K^+]$ C₅H₁₀Mo₂NO₄S₅ (m/z 503.7322), found m/z 503.7327. Anal. Calcd for C₅H₁₂KMo₂NO₅S₅: C, 10.77%; H, 2.17%; N, 2.51%. Found: C, 10.10%; H, 1.92%; N, 2.12%. $[\alpha]_D^{25}$ (DMF): -11.5° .

$K[(C_4H_8NO_3)Mo_2O_2(\mu-S)_2(S_2)] \cdot H_2O$ (**3**). $[(DMF)_3Mo_2O_2(\mu-S)_2(S_2)]$ (1.09 g, 1.91 mmol) and **3a** (0.33 g, 1.91 mmol) were placed in a Schlenk flask under N₂. Freshly distilled DMF (100 mL) was added to the flask via cannula. The reaction was stirred for 20 h. The clear red solution was filtered, and the solvent was removed under reduced pressure. The red viscous product was stirred in diethyl ether (100 mL) until it solidified. The solid was collected by filtration and redissolved in water (100 mL). The solution was filtered and lyophilized. This was repeated until all residual DMF was removed. The product was an orange solid (0.87 g, 90%). UV-vis (H₂O, 5.92×10^{-5} M), λ_{max} (nm): 274 (11858 M⁻¹ cm⁻¹), 305 (10233 M⁻¹ cm⁻¹), 347 (6402 M⁻¹ cm⁻¹), 474 (577 M⁻¹ cm⁻¹). 1H NMR (D₂O): δ ppm 4.26 (m, $-CH(OH)-$), 3.60 (br, $-CH(NH_2)-$), 1.33 (d, $-CH_3$). ^{13}C NMR (D₂O): δ ppm 172.62 ($-COO^-$), 65.82 ($-CH(OH)-$), 60.31 ($-CH(NH_2)-$), 19.39 ($-CH_3$). IR (KBr pellet, cm⁻¹): 3291 (m), 3220 (m), 3126 (m), 1625 (s), 1385 (m), 942 (s), 520 (w), 466 (m). MS-ESI: $[M - K^+]$ C₄H₈Mo₂NO₅S₄ (m/z 473.7393), found m/z 473.7399. Anal. Calcd for

C₄H₁₀KMo₂NO₆S₄: C, 9.11%; H, 1.91%; N, 2.66%. Found: C, 8.90%; H, 1.78%; N, 2.45%. $[\alpha]_D^{25}$ (DMSO): $+27.6^\circ$.

$K[(C_3H_6NO_3)Mo_2O_2(\mu-S)_2(S_2)] \cdot 1.5H_2O$ (**4**). $[(DMF)_3Mo_2O_2(\mu-S)_2(S_2)]$ (0.72 g, 1.26 mmol) and **4a** (0.18 g, 1.26 mmol) were placed in a Schlenk flask under N₂. Freshly distilled DMF (60 mL) was added to the flask via cannula. The reaction was stirred for 18 h. The clear red solution was filtered, and the solvent was removed under reduced pressure. The red viscous product was stirred in diethyl ether (100 mL) until it solidified. The solid was collected by filtration and redissolved in water (60 mL). The solution was filtered and lyophilized. This was repeated until all residual DMF was removed. The product was an orange solid (0.51 g, 78%). UV-vis (H₂O, 6.43×10^{-5} M), λ_{max} (nm): 275 (14275 M⁻¹ cm⁻¹), 305 (12720 M⁻¹ cm⁻¹), 347 (9029 M⁻¹ cm⁻¹), 474 (671 M⁻¹ cm⁻¹). 1H NMR (D₂O): δ ppm 4.00 (m, $-CH_2-$), 3.89 (br, $-CH(NH_2)-$). ^{13}C NMR (D₂O): δ ppm 172.16 ($-COO^-$), 60.11 ($-CH_2-$), 56.29 ($-CH(NH_2)-$). IR (KBr pellet, cm⁻¹): 3294 (m), 3224 (m), 3136 (m), 1617 (s), 1385 (m), 945 (s), 519 (w), 467 (m). MS-ESI: $[M - K^+]$ C₃H₆Mo₂NO₅S₄ (m/z 459.7237), found m/z 459.7231. Anal. Calcd for C₃H₉KMo₂NO_{6.5}S₄: C, 6.90%; H, 1.74%; N, 2.68%. Found: C, 6.40%; H, 1.72%; N, 2.60%. $[\alpha]_D^{25}$ (DMSO): $+55.9^\circ$.

$[Mo_2O_2(\mu-S)_2(\mu_2-C_6H_{12}NO_2)(C_6H_{12}NO_2)] \cdot 2H_2O$ (**5**). $[Mo_2O_2(\mu-S)_2(DMF)_6](I)_2$ (2.23 g, 2.27 mmol) was dissolved in acetone (40 mL) to form a red solution. L-C₆H₁₂NO₂ (0.60 g, 4.54 mmol) and NaOH (0.18 g, 4.54 mmol) were dissolved in H₂O (10 mL) and added dropwise to the red solution. The solution turned orange and cloudy. Acetone (40 mL) was added to the reaction, and the solution became clear. The reaction was stirred for 4 h. The solvent was removed under reduced pressure. The orange solid was stirred in H₂O (10 mL). The solid was isolated via filtration, and the red filtrate was discarded. The product was dissolved in ethanol (250 mL) and precipitated with diethyl ether (600 mL). The precipitate that formed was isolated via filtration. The orange filtrate was collected, the solvent was reduced to 20 mL, and product was further precipitated with diethyl ether (100 mL). The product was an orange solid (0.83 g, 73%). Single crystals suitable for X-ray analysis were obtained by recrystallization from methanol at gentle heating (50 °C). Needles formed upon the slow cooling of the solution. UV-vis (H₂O, 1.20×10^{-4} M), λ_{max} (nm): 281 (7393 M⁻¹ cm⁻¹), 350 (1786 M⁻¹ cm⁻¹). 1H NMR (DMSO- d_6): δ ppm 1.88 (m, $-CH(NH_2)-$), 1.01 (m, $(CH_3)_2-$), 0.95 (m, $(CH_3)_2CHCH_2-$), 0.66 (m, $(CH_3)_2-$). ^{13}C NMR (DMSO- d_6): δ ppm 181.85, 181.14, 99.53, 53.15, 52.90, 52.02, 41.70, 24.07, 23.99, 23.91, 23.50, 23.45, 23.20, 23.09, 21.95, 21.76, 21.42, 21.38. IR (KBr pellet, cm⁻¹): 3225 (m), 3169 (m), 3137 (m), 3062 (m), 1655 (s), 1617 (s), 1575 (m), 1389 (m), 1377 (m), 952 (s), 943 (s), 464 (m). MS-ESI: $[M - H^+]$ C₁₈H₃₆Mo₂N₃O₈S₂ (m/z 682.0052), found m/z 682.0057; $[M - C_6H_{11}NO_2]$ C₁₂H₂₃Mo₂N₂O₆S₂ (m/z 550.9106), found m/z 550.9111. Anal. Calcd for C₁₈H₄₁Mo₂N₃O₁₀S₂: C, 30.21%; H, 5.78%; N, 5.87%. Found: C, 30.30%; H, 5.42%; N, 5.87%. $[\alpha]_D^{25}$ (DMF): -22.4° .

$[Mo_2O_2(\mu-S)_2(C_5H_{10}NO_2S)] \cdot 0.5H_2O$ (**6**). $[Mo_2O_2(\mu-S)_2(DMF)_6](I)_2$ (2.32 g, 2.36 mmol) was dissolved in acetone (40 mL), forming a red solution. L-C₅H₁₀NO₂S (0.70 g, 4.72 mmol) and NaOH (0.19 g, 4.72 mmol) were dissolved in H₂O (20 mL) and added dropwise to the solution. The solution turned orange. The reaction was stirred for 20 h. The solution was filtered, and the solvent was reduced to 20 mL under reduced pressure. The orange precipitate that formed was isolated via filtration, redissolved in MeOH/DMF (100:50 mL), and precipitated with isopropyl alcohol (200 mL). The orange precipitate that formed was redissolved in acetone/H₂O (100:10 mL) and precipitated with diethyl ether (200 mL). The product was an orange solid (0.59 g, 42%). UV-vis (H₂O, 7.40×10^{-5} M), λ_{max} (nm): 284 (9550 M⁻¹ cm⁻¹), 350 (2152 M⁻¹ cm⁻¹). 1H NMR (D₂O): δ ppm 3.86 (t, $-CH(NH_2)-$), 2.65 (t, $-SCH_2CH_2-$), 2.20 (m, $-SCH_2CH_2-$), 2.15 (s, $-CH_3$). ^{13}C NMR (D₂O): δ ppm 174.15 ($-COO^-$), 53.89 ($-CH(NH_2)-$), 29.65 ($-SCH_2CH_2-$), 28.82 ($-SCH_2CH_2-$), 13.92 ($-CH_3$). IR (KBr pellet, cm⁻¹): 3223 (m, br), 3126 (m), 1644 (s), 1374 (m), 944 (s), 464 (m). MS-ESI: $[M - H^+]$ C₁₀H₁₉Mo₂N₂O₆S₄ (m/z 586.82), found m/z 586.82. Anal. Calcd for C₁₀H₂₁Mo₂N₂O_{6.5}S₄: C, 20.14%; H, 3.55%; N, 4.70%. Found: C, 20.41%; H, 3.72%; N, 4.03%. $[\alpha]_D^{25}$ (DMF): -53.7° .

[Mo₂O₂(μ-S)₂(C₄H₈NO₃)₂·H₂O] (7). [Mo₂O₂(μ-S)₂(DMF)₆](I)₂ (1.04 g, 1.06 mmol) was dissolved in H₂O (30 mL) to give a red solution. Ag[C₄H₈NO₃] (0.48 g, 2.12 mmol) was dissolved in H₂O (10 mL) and added dropwise to the red solution. The AgI precipitate started forming immediately. The reaction was stirred for 20 h. The precipitate was filtered off and discarded. The solvent of the filtrate was reduced to 20 mL under reduced pressure. Acetone (100 mL) and diethyl ether (100 mL) were added to the solution. The resulting precipitate was isolated via filtration. The solid was redissolved in H₂O (3 mL) and precipitated with acetone (100 mL) and diethyl ether (100 mL). The solid was redissolved in H₂O (3 mL) and lyophilized. The product was an orange powder (0.35 g, 61%). UV-vis (H₂O, 1.43 × 10⁻⁴ M), λ_{max} (nm): 281 (6528 M⁻¹ cm⁻¹), 350 (1498 M⁻¹ cm⁻¹). ¹H NMR (D₂O): δ ppm 4.17 (m, -CH(OH)-), 3.51 (br, -CH(NH₂)-), 1.33 (m, -CH₃). ¹³C NMR (D₂O): δ ppm 172.52 (-COO-), 65.78 (-CH(OH)-), 60.21 (-CH(NH₂)-), 19.36 (-CH₃). IR (KBr pellet, cm⁻¹): 3288 (m, br), 3129 (m), 1640 (s), 1382 (m), 943 (s), 464 (m). MS-ESI: [M - H⁺]⁻ C₈H₁₅Mo₂N₂O₈S₂ (m/z 526.8378), found m/z 526.8383. Anal. Calcd for C₈H₁₈Mo₂N₂O₉S₂: C, 17.72%; H, 3.35%; N, 5.17%. Found: C, 18.10%; H, 3.59%; N, 5.14%. [α]_D²⁵ (DMSO): -6.5°.

[Mo₂O₂(μ-S)₂(C₃H₆NO₃)₂] (8). [Mo₂O₂(μ-S)₂(DMF)₆](I)₂ (1.43 g, 1.46 mmol) and Ag[C₃H₆NO₃] (0.62 g, 2.92 mmol) were dissolved in H₂O (200 mL). The reaction was stirred for 20 h. A light-colored precipitate formed from the orange-colored solution. The AgI precipitate was filtered off and discarded. The filtrate was dried under reduced pressure. The resulting viscous oil was redissolved in H₂O (3 mL) and precipitated with acetone (100 mL). The solid was redissolved in H₂O (20 mL) and precipitated with acetone (200 mL). The product was collected by filtration, redissolved in H₂O (100 mL) and lyophilized. The product was an orange solid (0.44 g, 59%). UV-vis (H₂O, 1.58 × 10⁻⁴ M), λ_{max} (nm): 281 (5830 M⁻¹ cm⁻¹), 350 (1426 M⁻¹ cm⁻¹). ¹H NMR (D₂O): δ ppm 3.99 (m, -CH₂-), 3.89 (br, -CH(NH₂)-). ¹³C NMR (D₂O): δ ppm 172.07 (-COO-), 60.06 (-CH₂-), 56.22 (-CH(NH₂)-). IR (KBr pellet, cm⁻¹): 3211 (m, br), 3120 (m), 1617 (s), 1385 (m), 941 (s), 460 (m). MS-ESI: [M - H⁺]⁻ C₆H₁₁Mo₂N₂O₈S₂ (m/z 498.81), found m/z 498.81. Anal. Calcd for C₆H₁₂Mo₂N₂O₈S₂: C, 14.52%; H, 2.44%; N, 5.65%. Found: C, 14.76%; H, 2.41%; N, 5.76%.

Stoichiometric Reactions. Triplicate solutions containing the catalyst (1 mM) were prepared in veronal buffer (pH 7.4) along with a fourth one used as a blank solution that contained the same concentrations of the catalyst in veronal buffer. At *t* = 0, an amount of potassium cyanide (in 1.6 g/L NaOH/H₂O) was added to the three stock solutions so that the resulting concentration of cyanide would be 10 mM. An equivalent volume of NaOH (1.6 g/L H₂O) was added to the blank solution. Aliquots were removed from each of the three reaction solutions at time points *t* = 1, 3, 5, 10, 15, 20, 40, 60, and 120 min. To the aliquots was added to 2.5 mL of Fe(NO₃)₃ (0.2 M), and the solutions were diluted to 10 mL with HNO₃ (1 M). The absorptions of the resulting solutions were subsequently measured at 447 nm, and concentrations were calculated using a calibration curve for absorbance versus concentration of FeSCN²⁺.

Cytotoxicity. The cytotoxicity was determined using the MTT assay method previously described.⁹⁰ The assay measures the extent of the cellular reduction of 3-(4,5-dimethylthiazol-2-yl)-2,5-diphenyltetrazolium bromide (MTT) to a purple formazan product by the mitochondrial dehydrogenase of viable cells. First, 100 μL aliquots containing approximately 1 × 10⁴ A549 lung cancer cells per milliliter of the cell culture medium (advanced DMEM supplemented with 2% (v/v) fetal bovine serum and 1% (w/v) glutamine) was seeded in the wells of a 96-well plate (Costar) and allowed to adhere for 24 h at 37 °C in 5% (v/v) CO₂. The cell growth medium was then removed from the wells and replaced with solutions of the molybdenum or cisplatin complexes, which had been dissolved and then diluted in the culture medium such that 10 different concentrations ranging from 0 to 1000 μM for the molybdenum complexes and from 0 to 500 μM for cisplatin were obtained. Then, 100 μL of each drug concentration was added to six wells, and the cells were incubated for 72 h. Following incubation, MTT (20 mL, 2.5 mg mL⁻¹ in Milli Q water) was added to each well, and the plate was incubated for a further 4 h. The medium was removed, and

DMSO (dimethyl sulfoxide) (150 μL) was added to each well. The plate was shaken for 60 s, and the absorbance due to the formazan product was measured immediately at 600 nm using a Victor3 V plate reader (PerkinElmer). IC₅₀ values were determined as the drug concentration that reduced the absorbance to 50% of the value of the untreated control wells.

Catalytic Reactions. An analogous method was used as for the stoichiometric reactions. Thiosulfate was added to the complex solution in the desired quantity. The data workup calculated the thiocyanate concentration from the measured absorbance and plotted the [SCN⁻] versus time for several ratios of the thiosulfate to cyanide concentration. The conversion of cyanide was calculated based on found [SCN⁻] concentration versus the initial cyanide concentration, [CN⁻]₀.

Cyclic Voltammetry. The cyclic voltammetry data were recorded using a BASi Epsilon Eclipse electrochemical analyzer under nitrogen. CH₃CN solutions were prepared from distilled and degassed solvent and were 0.2 M in Bu₄NPF₆. The electrochemical cell used platinum working and auxiliary electrodes and a Ag/AgCl reference electrode.

X-ray Crystallography Data Collection. X-ray quality single crystals of **5** were obtained by recrystallization in MeOH (50 °C) and slow cooling at 21 °C. The crystals were isolated from the mother liquor, immediately immersed in a cryogenic oil, and then mounted. The X-ray single crystal data were collected using Cu Kα radiation (λ = 1.54178 Å) on a Bruker D8Venture (Photon100 CMOS detector) diffractometer equipped with Cryostream (Oxford Cryosystems) open-flow nitrogen cryostats at 120.0(2) K. The unit cell determination, data collection, data reduction, structure solution and refinement, and empirical absorption correction (SADABS) were carried out using Apex3 software.⁹¹ The structure was solved by the direct method and refined by full-matrix least-squares on F² for all data using SHELXTL⁹² software. The final refinements were performed using TWIN and BASF instructions,⁹³ and the structure was refined as a two-component inversion. The carbon atom of one of the methanol molecules was disordered, and the free variables were refined by FVAR instruction. All nonordered non-hydrogen atoms were refined anisotropically. We were not able to refine the hydrogen atoms of the nitrogen atom located in the Fourier map to a proper model. Thus, all the hydrogen atoms were placed in the calculated positions and refined in the riding model.

X-ray-quality single crystals of **9** were obtained by the dissolution of **8** in acetonitrile with 2 equiv of Bu₄NSCN and KSCN and layering with ether. A suitable crystal was selected and placed in paratone on a micromount on a Bruker SMART APEXII diffractometer equipped with a CCD area detector. The crystal was kept at 100(2) K during data collection. Using Olex2,⁹⁴ the structure was solved with the olex2.solve structure solution program⁹⁵ using charge flipping and refined with the ShelXL refinement package⁹⁶ using least-squares minimization. The structure had a number of issues that were dealt with during refinement. First, the tetra-*n*-butyl ammonium cation is disordered across a two-fold rotation axis; chemically equivalent bond lengths and angles of the cation were restrained to be approximately equal. The acetonitrile solvent molecule is disordered across a 3.2 site (Wyckoff letter c). Due to the very low occupancy in the asymmetric unit, the 1,2- and 1,3-distances of this molecule were restrained to ideal values from the CSD. The CH₃ group of this also would not find a minimum during refinement, so a distance restraint was applied between one of these atoms and an atom on the adjacent *n*-Bu₄N cation. This molecule could not be sensibly refined anisotropically and so was refined isotropically. The second potassium cation is disordered over two positions. The occupancies of these two positions were refined competitively, converging to a ratio of 0.23:0.10. The water molecule is half-occupied and additionally disordered around a three-fold rotation axis. The hydrogen atoms could not be sensibly located or modeled and so were excluded from the model; however, they were included in the formula and the calculation of derived parameters. Finally, enhanced rigid bond and similarity restraints were applied to the thermal parameters of all non-hydrogen atoms. Further crystallographic details are provided in the tables in the Supporting Information.

■ ASSOCIATED CONTENT

SI Supporting Information

The Supporting Information is available free of charge at <https://pubs.acs.org/doi/10.1021/acs.inorgchem.0c02672>.

Summary of crystal data, bond angles, and distances for **5** and **9**; ESI-MS spectra of **1–8**; cytotoxicity results; cyclic voltammetry traces **1–8**; and catalytic activity of bis-amino acid complexes(PDF)

Accession Codes

CCDC 2027204–2027205 contain the supplementary crystallographic data for this paper. These data can be obtained free of charge via www.ccdc.cam.ac.uk/data_request/cif, or by emailing data_request@ccdc.cam.ac.uk, or by contacting The Cambridge Crystallographic Data Centre, 12 Union Road, Cambridge CB2 1EZ, UK; fax: +44 1223 336033.

■ AUTHOR INFORMATION

Corresponding Author

Sigrídur G. Suman – Science Institute, University of Iceland, 107 Reykjavík, Iceland; orcid.org/0000-0003-4283-6140; Email: sgsuman@hi.is

Authors

Johanna M. Gretarsdóttir – Science Institute, University of Iceland, 107 Reykjavík, Iceland

Sigrídur Jonsdóttir – Science Institute, University of Iceland, 107 Reykjavík, Iceland

William Lewis – School of Chemistry, The University of Sydney, Sydney, NSW 2006, Australia; orcid.org/0000-0001-7103-6981

Trevor W. Hambley – School of Chemistry, The University of Sydney, Sydney, NSW 2006, Australia; orcid.org/0000-0003-1194-1896

Complete contact information is available at:

<https://pubs.acs.org/doi/10.1021/acs.inorgchem.0c02672>

Author Contributions

All authors have given approval to the final version of the manuscript.

Notes

The authors declare the following competing financial interest(s): S.G. Suman is the author of published patents describing treatment for cyanide poisoning using molybdenum compounds.

Hydrogen cyanide is volatile and highly toxic. To minimize exposure, cyanide stock solutions were prepared in 40 mM NaOH and diluted to the desired concentrations in veronal buffer.

■ ACKNOWLEDGMENTS

Prof. K. K. Damodaran is thanked for crystal data collection and the refinement of **5**. Financial support by The University of Iceland Research Fund and from The Icelandic Centre of Research (Rannis) grant 140945 are gratefully acknowledged.

■ REFERENCES

- (1) Lawson-Smith, P.; Jansen, E. C.; Hyldegaard, O. Cyanide intoxication as part of smoke inhalation—a review on diagnosis and treatment from the emergency perspective. *Scand. J. Trauma Resusc.* **2011**, *19*, 14.
- (2) Suman, S. G.; Gretarsdóttir, J. M. Chemical and Clinical Aspects of Metal-Containing Antidotes for Poisoning by Cyanide. In *Essential*

Metals in Medicine: Therapeutic Use and Toxicity of Metal Ions in the Clinic; Sigel, A., Freisinger, E., Sigel, R. K. O., Carver, P. L., Eds.; Metal Ions in Life Sciences, Vol. 19; Walter de Gruyter: Berlin, Germany, 2019; pp 359–391

(3) Ma, J.; Dasgupta, P. K. Recent developments in cyanide detection: a review. *Anal. Chim. Acta* **2010**, *673* (2), 117–25.

(4) Maniscalco, P. M. From Smoke Inhalation to Chemical Attacks: Acute Cyanide Poisoning in the Prehospital Setting. *Prehosp. Disaster Med.* **2006**, *21* (2), S38–S39.

(5) Alarie, Y. Toxicity of Fire Smoke. *Crit. Rev. Toxicol.* **2002**, *32* (4), 259–289.

(6) Megarbane, B.; Delahaye, A.; Goldgran-Toledano, D.; Baud, F. J. Antidotal Treatment of Cyanide Poisoning. *J. Chin. Med. Assoc.* **2003**, *66*, 193–203.

(7) Alarie, Y. The Toxicity of Smoke from Polymeric Materials during Thermal Decomposition. *Annu. Rev. Pharmacol. Toxicol.* **1985**, *25*, 325–347.

(8) Environmental Health Center A. *Cyanide Compounds Chemical Background*; Environmental Health Center A, Division of the National Safety Council: Washington, D.C., 1997.

(9) Mediavilla, J. J. V.; Perez, B. F.; Cordoba, M. C. F. d.; Espina, J. A.; Ania, C. O. Photochemical Degradation of Cyanides and Thiocyanates from an Industrial Wastewater. *Molecules* **2019**, *24*, 1373.

(10) Betancourt-Buitrago, L. A.; Hernandez-Ramirez, A.; Colina-Marquez, J. A.; Bustillo-Lecompte, C. F.; Rehmann, L.; Machuca-Martinez, F. Recent Developments in the Photocatalytic Treatment of Cyanide Wastewater: An Approach to Remediation and Recovery of Metals. *Processes* **2019**, *7*, 225.

(11) Borron, S. W.; Baud, F. J. Acute Cyanide Poisoning: Clinical Spectrum, Diagnosis, and Treatment. *Arh. Hig. Rada. Toksikol.* **1996**, *47* (3), 307–322.

(12) Hall, A. H.; Saisers, J.; Baud, F. Which cyanide antidote? *Crit. Rev. Toxicol.* **2009**, *39* (7), 541–552.

(13) Allen, A. R.; Booker, L.; Rockwood, G. A., Acute Cyanide Toxicity. In *Toxicology of Cyanides and Cyanogens: Experimental, Applied and Clinical Aspects*, 1st ed.; Hall, A. H., Isom, G. E., Rockwood, G. A., Eds; John Wiley & Sons, Ltd.: Chichester, U.K., 2015; p 20.

(14) Patterson, S. E.; Moeller, B.; Nagasawa, H. T.; Vince, R.; Crankshaw, D. L.; Briggs, J.; Stutelberg, M. W.; Vinnakota, C. V.; Logue, B. A. Development of Sulfanegen for Mass Cyanide Casualties. *Ann. N. Y. Acad. Sci.* **2016**, *1374*, 202–209.

(15) Brenner, M.; Kim, J. G.; Mahon, S. B.; Lee, J.; Kreuter, K. A.; Blackledge, W.; Mukai, D.; Patterson, S.; Mohammad, O.; Sharma, V. S.; Boss, G. R. Intramuscular cobinamide sulfite in a rabbit model of sublethal cyanide toxicity. *Ann. Emerg. Med.* **2010**, *55* (4), 352–63.

(16) Gunasekar, P. G.; Borowitz, J. L.; Turek, J. J.; Van Horn, D. A.; Isom, G. E. Endogenous Generation of Cyanide in Neuronal Tissue: involvement of a Peroxidase System. *J. Neurosci. Res.* **2000**, *61*, 570–575.

(17) Huang, J.; Niknahad, H.; Khan, S.; O'Brien, P. J. Hepatocyte-Catalysed Detoxification of Cyanide by L- and D-Cysteine. *Biochem. Pharmacol.* **1998**, *55*, 1983–1990.

(18) Ivankovich, A. D.; Braverman, B.; Kanuru, R. P.; Heyman, H. J.; Paulsian, R. Cyanide Antidotes and Methods of their Administration in Dogs: A Comparison Study. *Anesthesiology* **1980**, *52*, 210–216.

(19) Soldevila-Barreda, J. J.; Sadler, P. J. Approaches to the design of catalytic metallo-drugs. *Curr. Opin. Chem. Biol.* **2015**, *25*, 172–183.

(20) Gasser, G.; Ott, I.; Metzler-Nolte, N. Organometallic anticancer compounds. *J. Med. Chem.* **2011**, *54* (1), 3–25.

(21) Gretarsdóttir, J. M.; Bobersky, S.; Metzler-Nolte, N.; Suman, S. G. Cytotoxicity studies of water soluble coordination compounds with a [Mo₂O₂S₂]²⁺ core. *J. Inorg. Biochem.* **2016**, *160*, 166–171.

(22) Enemark, J. H.; Cooney, J. A.; Wang, J.-J.; Holm, R. H. Synthetic Analogues and Reaction Systems Relevant to the Molybdenum and Tungsten Oxotransferases. *Chem. Rev.* **2004**, *104*, 1175–1200.

(23) Coucouvanis, D. Functional analogs for the reduction of certain nitrogenase substrates. Are multiple sites within the Fe/Mo/S active center involved in the 6e⁻ reduction of N₂? *J. Biol. Inorg. Chem.* **1996**, *1*, 594–600.

- (24) Hille, R. Molybdenum and Tungsten in Biology. *Trends Biochem. Sci.* **2002**, *27* (7), 360–368.
- (25) *Molybdenum and Tungsten: Their Roles in Biological Processes*, 1st ed.; Sigel, A.; Sigel, H., Eds.; Metal Ions in Biological Systems, Vol. 39; Taylor & Francis Group: Boca Raton, FL, 2002.
- (26) Hille, R. Molybdenum-containing hydroxylases. *Arch. Biochem. Biophys.* **2005**, *433* (1), 107–116.
- (27) Daage, M.; Chianelli, R. R. Structure-function relations in molybdenum sulfide catalysts: The “Rim-Edge” model. *J. Catal.* **1994**, *149* (2), 414–427.
- (28) Abdalghani, I.; Biancalana, L.; Aschi, M.; Pampaloni, G.; Marchetti, F.; Crucianelli, M. Dioxomolybdenum(VI) compounds with α -amino acid donor ligands as catalytic precursors for the selective oxyfunctionalization of olefins. *Mol. Catal.* **2018**, *446*, 39–48.
- (29) Smith, P. D.; Slizys, D. A.; George, G. N.; Young, C. G. Toward a Total Model for the Molybdenum Hydroxylases: Synthesis, Redox, and Biomimetic Chemistry of Oxo-thio-Mo(VI) and -Mo(V) Complexes. *J. Am. Chem. Soc.* **2000**, *122*, 2946–2947.
- (30) Kim, C. G.; Coucouvanis, D. Reactions of the Mo = S Bond in the [(Cp)Mo(O)(μ -S)2Mo(O)(S)]₂ complex with SO₂. An IH NMR Study and the Synthesis and Structural Characterization of [(Cp)Mo(O)(μ -S)2Mo(O)(L)]₂ Complexes Containing SO₂-Derived Sulfite, Thiosulfate, and Sulfate Bidentate Chelating Ligands. *Inorg. Chem.* **1993**, *32*, 1881–1882.
- (31) Young, C. G. Models for the molybdenum hydroxylases. *JBIC, J. Biol. Inorg. Chem.* **1997**, *2* (2), 810.
- (32) Coughlan, M. P.; Johnson, J. L.; Rajagopalan, K. V. Mechanisms of inactivation of molybdoenzymes by cyanide. *J. Biol. Chem.* **1980**, *255* (7), 2694–2699.
- (33) Stiefel, E. I. The coordination and bioinorganic chemistry of molybdenum. *Prog. Inorg. Chem.* **2007**, *22*, 1–223.
- (34) Doonan, C. J.; Gourlay, C.; Nielsen, D. J.; Ng, V. W.; Smith, P. D.; Evans, D. J.; George, G. N.; White, J. M.; Young, C. G. d(1) Oxosulfido-Mo(V) Compounds: First Isolation and Unambiguous Characterization of an Extended Series. *Inorg. Chem.* **2015**, *54* (13), 6386–96.
- (35) Young, C. G. 4.7 Molybdenum. *Comprehensive Coordination Chemistry II* **2003**, *4*, 415–527.
- (36) Mitchell, P. C. H.; Pygall, C. F. Reactions of Molybdenum-Sulfur Compounds with Cyanide: Chemical Evolution and Deactivation of Molybdoenzymes. *J. Inorg. Biochem.* **1979**, *11*, 25–29.
- (37) Drew, M. G. B.; Mitchell, P. C. H.; Pygall, C. F. Reaction between Molybdate(VI), Cyanide, and Hydrogen Sulfide. *Angew. Chem., Int. Ed. Engl.* **1976**, *15* (12), 784–785.
- (38) Suman, S. G.; Gretarsdottir, J. M.; Penwell, P. E.; Gunnarsson, J. P.; Frostason, S.; Jonsdottir, S.; Damodaran, K. K.; Hirschon, A. Reaction Chemistry of the syn-[Mo₂O₂(μ -S)₂(S₂)(DMF)₃] Complex with Cyanide and Catalytic Thiocyanate Formation. *Inorg. Chem.* **2020**, *59* (11), 7644–7656.
- (39) Rodgers, M. T.; Armentrout, P. B.; Oomens, J.; Steill, J. D. Infrared Multiphoton Dissociation Spectroscopy of Cationized Threonine: Effects of Alkali-Metal Cation Size on Gas-Phase Conformation. *J. Phys. Chem. A* **2008**, *112* (11), 2258–2267.
- (40) Armentrout, P. B.; Rodgers, M. T.; Oomens, J.; Steill, J. D. Infrared Multiphoton Dissociation Spectroscopy of Cationized Serine: Effects of Alkali-Metal Cation Size on Gas-Phase Conformation. *J. Phys. Chem. A* **2008**, *112* (11), 2248–2257.
- (41) Ye, S. J.; Armentrout, P. B. Experimental and Theoretical Investigation of the Decomposition of Lithiated Hydroxyl Side-Chain Amino Acids. *J. Phys. Chem. B* **2008**, *112* (33), 10303–10313.
- (42) Carl, D. R.; Cooper, T. E.; Oomens, J.; Steill, J. D.; Armentrout, P. B. Infrared multiple photon dissociation spectroscopy of cationized methionine: effects of alkali-metal cation size on gas-phase conformation. *Phys. Chem. Chem. Phys.* **2010**, *12* (14), 3384–3398.
- (43) Armentrout, P. B.; Gabriel, A.; Moision, R. M. An experimental and theoretical study of alkali metal cation/methionine interactions. *Int. J. Mass Spectrom.* **2009**, *283* (1), 56–68.
- (44) Cao, X.; Fischer, G. Conformational and Infrared Spectral Studies of L-Methionine and Its N-Deuterated Isotopomer as Isolated Zwitterions. *J. Phys. Chem. A* **2002**, *106* (1), 41–50.
- (45) Kay, A.; Mitchell, P. C. H. Molybdenum–Cysteine Complex. *Nature* **1968**, *219* (5151), 267–268.
- (46) Shibahara, T.; Akashi, H.; Toupadakis, A.; Coucouvanis, D. Sulfur-bridged dinuclear molybdenum(V) complexes with Mo₂O₃S and Mo₂O₂S₂ cores. *Inorganic Synthesis* **2007**, *29*, 254–260.
- (47) Ott, V. R.; Swieter, D. S.; Schultz, F. A. Di- μ -oxo, μ -Oxo- μ -sulfido, and Di- μ -sulfido Complexes of Molybdenum(V) with EDTA, Cysteine, and Cysteine Ester Ligands. Preparation and Electrochemical and Spectral Properties. *Inorg. Chem.* **1977**, *16* (10), 2538–2545.
- (48) Sokolov, M. N.; Adonin, S. A.; Virovets, A. V.; Abramov, P. A.; Vicent, C.; Llusar, R.; Fedin, V. P. Complexes of M₃S₄⁺ (M = Mo, W) with chiral α -hydroxy and aminoacids: Synthesis, structure and solution studies. *Inorg. Chim. Acta* **2013**, *395*, 11–18.
- (49) Wu, J.-F.; Li, D.-M.; Cui, L.-F.; Zhuang, C.-F.; Song, S.-N.; Wang, T.-G.; Xu, J.-Q.; Jia, H.-Q.; Hu, N.-H. Two novel molybdenum complexes containing [Mo₂O₂S₂]₂⁺ fragment: synthesis, crystal structures and catalytic studies. *Appl. Organomet. Chem.* **2007**, *21* (12), 1033–1040.
- (50) Murphy, J. M.; Powell, B. A.; Brumaghim, J. L. Stability constants of bio-relevant, redox-active metals with amino acids: The challenges of weakly binding ligands. *Coord. Chem. Rev.* **2020**, *412*, 213253–21.
- (51) Inklaar, P. A. Methods for Preparing Solid Salts of Amino Acids. US 3450752 A, 1969.
- (52) Coucouvanis, D.; Toupadakis, A.; Lane, J. D.; Koo, S. M.; Kim, C. G.; Hadjikyriacou, A. Reactivity of the Mo(O)(S) functional group in the [(L)Mo(O)(μ -S)2Mo(O)(S)]_n-dimeric thiomolybdate complexes, (L = C₅H₅—, n = 1; S₄²⁻, n = 2) and implications regarding the function of xanthine oxidase. Synthesis and structural characterization of [(DMF)₃Mo(O)(μ -S)2Mo(O)(S₂)], [Ph₄P][[(C₅H₅)Mo(O)(μ -S)2Mo(O)(S₂)], [Ph₄P]2[(S₄)Mo(O)(μ -S)2Mo(O)(S)] and (Et₄N)₄[(S₄)Mo(O)(μ -S)2Mo(O)(S)]₂. *J. Am. Chem. Soc.* **1991**, *113* (14), 5271–5282.
- (53) Singh, R.; Whitesides, G. M., Thiol–Disulfide Interchange. In *Supplement S: The Chemistry of Sulfur-Containing Functional Groups*; Patai, S., Rappoport, Z., Ed.; The Chemistry of Functional Groups; John Wiley and Sons, Ltd.: Chichester, U.K., 1993; pp 633–658.
- (54) Coucouvanis, D.; Toupadakis, A.; Hadjikyriacou, A. Synthesis of thiomolybdenyl complexes with [Mo₂(S)₂(O)₂]₂⁺ cores and substitutionally labile ligands. Crystal and molecular structure of the tris(dimethylformamide)dioxotetrasulfidodimolybdenum complex. *Inorg. Chem.* **1988**, *27* (19), 3272–3273.
- (55) Coucouvanis, D.; Hadjikyriacou, A.; Toupadakis, A.; Koo, S. M.; Ieperuma, O.; Draganjac, M.; Salifoglou, A. Studies of the reactivity of binary thio- and tertiary oxothiomolybdates toward electrophiles. Reactions with dicarbomethoxyacetylene and the synthesis and structures of the [Et₄N]2[Mo(O)L₂], anti-[Et₄N]2[Mo₂O₂S₂(L)₂], syn-[Ph₄P]2[Mo₂O₂S₂(L)₂].cntdot.2DMF, Ph₄P]2[Mo(L)₃]-DMF.cntdot.C₆H₆, and [Ph₄P]2[Mo₂S₂(L)₄]2CH₂Cl₂ complexes (L = 1,2-dicarbomethoxy-1,2-ethylenedithiolate). *Inorg. Chem.* **1991**, *30* (4), 754–767.
- (56) Guggenheim, M. Complex Silver Salts of α -Amino Acids. US 1417167 A, 1922.
- (57) Severin, K.; Bergs, R.; Beck, W. Bioorganometallic Chemistry and Transition Metal Complexes with α -Amino Acids and Peptides. *Angew. Chem., Int. Ed.* **1998**, *37*, 1634–1654.
- (58) Berthon, G. Critical evaluation of the stability constants of metal complexes of amino acids with polar side chains (Technical Report). *Pure Appl. Chem.* **1995**, *67*, 1117.
- (59) Pettit, L. D.; Bezer, M. Complex formation between palladium(II) and amino acids, peptides and related ligands. *Coord. Chem. Rev.* **1985**, *61*, 97–114.
- (60) Yoshida, R.; Ogasahara, S.; Akashi, H.; Shibahara, T. Crystal structural diversity of sulfur-bridged cysteinato dimolybdenum(V)-complexes: The influence of counter metal cations. *Inorg. Chim. Acta* **2012**, *383*, 157–163.

- (61) Morgenstern, U.; Wagner, C.; Merzweiler, K. Dinuclear Molybdenum(II) Complexes with Thioether Functionalized Silylamide Ligands. *Z. Anorg. Chem.* **2010**, *646* (13), 642–647.
- (62) McAuliffe, C. A.; Quagliano, J. V.; Vallarino, L. M. Metal Complexes of the Amino Acid DL-Methionine. *Inorg. Chem.* **1966**, *5* (11), 1996–2003.
- (63) Raju, E. V.; Mathur, H. B. Transition Metal Complexes of Serine and Threonine. *J. Inorg. Nucl. Chem.* **1968**, *30*, 2181–2188.
- (64) Sarkar, B.; Bersohn, M.; Wigfield, Y.; Chiang, T.-C. Visible, optical rotatory dispersion, and paramagnetic resonance spectra of the L-histidine–Cu(II)–L-threonine complex. *Can. J. Biochem.* **1968**, *46* (6), 595–600.
- (65) Djordjevic, C.; Vuletic, N.; Jacobs, B. A.; Lee-Renslo, M.; Sinn, E. Molybdenum(VI) Peroxo α -Amino Acid Complexes: Synthesis, Spectra, and Properties of $\text{MoO}(\text{O}_2)_2(\alpha\text{-aa})(\text{H}_2\text{O})$ for $\alpha\text{-aa}$ = Glycine, Alanine, Proline, Valine, Leucine, Serine, Asparagine, Glutamine, and Glutamic Acid. X-ray Crystal Structures of the Glycine, Alanine, and Proline Compounds. *Inorg. Chem.* **1997**, *36* (9), 1798–1805.
- (66) Zhou, Z.-H.; Wan, H.-L.; Tsai, K.-R. Molybdenum(VI) complex with citric acid: synthesis and structural characterization of 1:1 ratio citrato molybdate $\text{K}_2\text{Na}_4[(\text{MoO}_2)_2(\text{cit})_2] \cdot 5\text{H}_2\text{O}$. *Polyhedron* **1997**, *16* (1), 75–79.
- (67) Clegg, W.; Mohan, N.; Mueller, A.; Neumann, A.; Rittner, W.; Sheldrick, G. M. Crystal and molecular structure of $[\text{N}(\text{CH}_3)_4]_2[\text{Mo}_2\text{O}_2\text{S}_2(\text{S}_2)_2]$: a compound with two S_2^{2-} ligands. *Inorg. Chem.* **1980**, *19* (7), 2066–2069.
- (68) Knox, J. R.; Prout, C. K. The Structure of a Cysteine Complex of Molybdenum(V): $\text{Na}_2\text{Mo}_2\text{O}_4[\text{SCH}_2\text{CH}(\text{NH}_2)(\text{CO}_2)] \cdot 2.5\text{H}_2\text{O}$. *Acta Crystallogr., Sect. B: Struct. Crystallogr. Cryst. Chem.* **1969**, *25*, 1857–1957.
- (69) Birgisson, B. O.; Monger, L. J.; Damodaran, K. K.; Suman, S. G. Synthesis and characterization of asymmetric $[\text{Mo}_2\text{O}_2(\mu\text{-S})_2(\text{S}_2)(\text{L})]$ complexes (L = bipy, en, dien) and their heterogeneous reaction with propylene sulfide. *Inorg. Chim. Acta* **2020**, *501*, 119272.
- (70) Nozaki, Y.; Tanford, C. The Solubility of Amino Acids and Related Compounds in Aqueous Ethylene Glycol Solutions. *J. Biol. Chem.* **1965**, *240* (9), 3568–3573.
- (71) Yao, H.; Xu, Z.; Li, C.; Tse, M.-K.; Tong, Z.; Zhu, G. Synthesis and Cytotoxic Study of a Platinum(IV) Anticancer Prodrug with Selectivity toward Luteinizing Hormone-Releasing Hormone (LHRH) Receptor-Positive Cancer Cells. *Inorg. Chem.* **2019**, *58* (16), 11076–11084.
- (72) Gretarsdottir, J. M. *Syntheses of New Molybdenum–Sulfur Complexes: Catalytic Transformation of Cyanide to Thiocyanate, and In Vitro Biological Studies*. PhD Dissertation, University of Iceland, Iceland, 2018.
- (73) Schultz, F. A.; Ott, V. R.; Rolison, D. S.; Bravard, D. C.; McDonald, J. W.; Newton, W. E. Synthesis and Electrochemistry of Oxo- and Sulfido-Bridged Molybdenum(V) Complexes with 1, 1-Dithiolate Ligands. *Inorg. Chem.* **1978**, *17* (7), 1758–1765.
- (74) Hijazi, A.; Kemmegne-Mbouguen, J. C.; Floquet, S.; Marrot, J.; Fize, J.; Artero, V.; David, O.; Magnier, E.; Pégot, B.; Cadot, E. Tuning the electrocatalytic hydrogen evolution reaction promoted by $[\text{Mo}_2\text{O}_2\text{S}_2]$ -based molybdenum cycles in aqueous medium. *Dalton Trans.* **2013**, *42* (14), 4848–4858.
- (75) Spivack, B.; Dori, Z. Separation and unusual stability of the sulphur-bridged ion $\text{Mo}_2\text{S}_2\text{O}_{22}^{+}$. *J. Chem. Soc., Chem. Commun.* **1973**, No. 23, 909–910.
- (76) Elgrishi, N.; McCarthy, B. D.; Rountree, E. S.; Dempsey, J. L. Reaction Pathways of Hydrogen-Evolving Electrocatalysts: Electrochemical and Spectroscopic Studies of Proton-Coupled Electron Transfer Processes. *ACS Catal.* **2016**, *6* (6), 3644–3659.
- (77) Schultz, F. A. Structure–reactivity relationships in inorganic electrochemistry. *J. Solid State Electrochem.* **2011**, *15* (7), 1833–1843.
- (78) Kuntz, R. R. Comparative Study of $\text{Mo}_2\text{O}_x\text{S}_y(\text{cys})_2$ -Complexes as Catalysts for Electron Transfer from Irradiated Colloidal TiO_2 to Acetylene. *Langmuir* **1997**, *13* (6), 1571–1576.
- (79) Smith, D. A.; Zhuang, B.; Newton, W. E.; McDonald, J. W.; Shultz, F. A. Two-electron transfer accompanied by metal-metal bond formation. Synthesis and electrochemistry of dinuclear molybdenum and tungsten carbonyl thiolates. *Inorg. Chem.* **1987**, *26* (15), 2524–2531.
- (80) Kemmegne-Mbouguen, J. C.; Floquet, S.; Zang, D.; Bonnefont, A.; Ruhlmann, L.; Simonnet-Jégat, C.; López, X.; Haouas, M.; Cadot, E. Electrochemical properties of the $[\text{SiW}_{10}\text{O}_{36}(\text{M}_2\text{O}_2\text{E}_2)]_6^-$ polyoxometalate series (M = Mo(v) or W(v); E = S or O). *New J. Chem.* **2019**, *43* (3), 1146–1155.
- (81) Adam, W.; Bargon, R. M.; Bosio, S. G.; Schenk, W. A.; Stalke, D. Direct Synthesis of Isothiocyanates from Isonitriles by Molybdenum-Catalyzed Sulfur Transfer with Elemental Sulfur. *J. Org. Chem.* **2002**, *67* (20), 7037–7041.
- (82) Hall, A. H.; Dart, R.; Bogdan, G. Sodium thiosulfate or hydroxocobalamin for the empiric treatment of cyanide poisoning? *Ann. Emerg. Med.* **2007**, *49* (6), 806–813.
- (83) Borron, S. W.; Baud, F. J.; Megarbane, B.; Bismuth, C. Hydroxocobalamin for severe acute cyanide poisoning by ingestion or inhalation. *Am. J. Emerg. Med.* **2007**, *25* (5), 551–8.
- (84) Baud, F. J. Cyanide: critical issues in diagnosis and treatment. *Hum. Exp. Toxicol.* **2007**, *26* (3), 191–201.
- (85) Suman, S. G.; Gretarsdottir, J. M.; Penwell, P. E.; Gunnarsson, J. P.; Frostason, S.; Jonsdottir, S.; Damodaran, K. K.; Hirschon, A. Reaction Chemistry of the $\text{syn-Mo}_2\text{O}_2(\mu\text{-S})_2(\text{S}_2)(\text{DMF})_3$ Complex with Cyanide and Catalytic Thiocyanate Formation. *Inorg. Chem.* **2020**, *59*, 7644.
- (86) Leininger, K. R.; Westley, J. The Mechanism of the Rhodanese-catalyzed Thiosulfate Cyanide Reaction. *J. Biol. Chem.* **1968**, *243* (8), 1892–1899.
- (87) Bamford, V. A.; Bruno, S.; Rasmussen, T.; Appia-Ayme, C.; Cheesman, M. R.; Berks, B. C.; Hemmings, A. M. Structural basis for the oxidation of thiosulfate by a sulfur cycle enzyme. *EMBO Journal* **2002**, *21* (21), 5599–5610.
- (88) Schlesinger, P.; Westley, J. An Expanded Mechanism for Rhodanese Catalysis. *J. Biol. Chem.* **1974**, *249* (3), 780–788.
- (89) Armarego, W. L. F. *Purification of Laboratory Chemicals*, 8th ed.; Butterworth-Heinemann: Cambridge, MA, 2017.
- (90) Carmichael, J.; DeGraff, W. G.; Gazdar, A. F.; Minna, J. D.; Mitchell, J. B. Evaluation of a tetrazolium-based semiautomated colorimetric assay: assessment of chemosensitivity testing. *Cancer Res.* **1987**, *47*, 936–942.
- (91) Apex3; Bruker AXS: Madison, WI, 2015.
- (92) Sheldrick, G. M. A short history of SHELX. *Acta Crystallogr., Sect. A: Found. Crystallogr.* **2008**, *64* (1), 112–122.
- (93) Sheldrick, G. M. Crystal structure refinement with SHELXL. *Acta Crystallogr., Sect. C: Struct. Chem.* **2015**, *71*, 3–8.
- (94) Dolomanov, O. V.; Bourhis, L. J.; Gildea, R. J.; Howard, J. A. K.; Puschmann, H. OLEX2: a complete structure solution, refinement and analysis program. *J. Appl. Crystallogr.* **2009**, *42*, 339–341.
- (95) Bourhis, L. J.; Dolomanov, O. V.; Gildea, R. J.; Howard, J. A. K.; Puschmann, H. The anatomy of a comprehensive constrained, restrained refinement program for the modern computing environment-Olex2 dissected. *Acta Crystallogr., Sect. A: Found. Adv.* **2015**, *71*, 59–75.
- (96) Sheldrick, G. M. Crystal structure refinement with SHELXL. *Acta Crystallogr., Sect. C: Struct. Chem.* **2015**, *71*, 3–8.